131) Aicardi J, Castelein P. Infantile neuroaxonal dystrophy. Brain. 1979; 102: 727-48.
132) Morgan NV, Westaway SK, Morton JE, et al. PLA2G6 encoding a phospholipase A2, is mutated in neurodegenerative disorders with high brain iron. Nat Genet. 2006; 38: 752-4.
133) Sina F, Shojaee S, Elahi E, et al. R632W mutation in PLA2G6 segregates with dystonia-parkinsonism in a consanguineous Iranian family. Eur J Neurol. 2009; 16: 101-4.
134) Yoshino H, Tomiyama H, Tachibana N, et al. Phenotypic spectrum of patients with *PLA2G6* mutation and *PARK14*-linked parkinsonism. Neurology. 2010; 75: 1356-61.
135) Di Fonzo A, Dekker MC, Montagna P, et al. FBXO7 mutations cause autosomal recessive, early-onset parkinsonian-pyramidal syndrome. Neurology. 2009; 72: 240-5.
136) Hicks AA, Pétursson H, Jónsson T, et al. A susceptibility gene for late-onset idiopathic Parkinson's disease. Ann Neurol. 2002; 52: 549-55.
137) Oliveira SA, Li Y-J, Noureddine MA, et al. Identification of risk and age-at-onset genes on chromosome 1p in Parkinson disease. Am J Hum Genet. 2005; 77: 252-64.
138) Noureddine MA, Qin X-J, Oliveira SA, et al. Association between the neuron-specific RNA-binding protein ELAVL4 and Parkinson disease. Hum Genet. 2005; 117: 27-33.
139) Haugarvoll K, Toft M, Ross OA, et al. ELAVL4, PARK10, and the Celts. Move Disord. 2007; 22: 585-7.
140) DeStefano AL, Latourelle J, Lew MF, et al. Replication of association between ELAVL4 and Parkinson disease: the GenePD study. Hum Genet. 2008; 124: 95-9.
141) Noureddine MA, Li YJ, van der Walt JM, et al. Genomic convergence to identify candidate genes for Parkinson disease: SAGE analysis of the substantia nigra. Mov Disord. 2005; 20: 1299-309.
142) Anderson LR, Betarbet R, Gearing M, et al. PARK10 candidate RNF11 is expressed by vulnerable neurons and localizes to Lewy bodies in Parkinson disease brain. J Neuropath Exp Neurol. 2007; 66: 955-64.
143) Pankratz N, Nichols WC, Uniacke SK, et al. Genome screen to identify susceptibility genes for Parkinson disease in a sample without parkin mutations. Am J Hum Genet. 2002; 71: 124-35.
144) Pankratz N, Nichols WC, Uniacke SK, et al. Genome-wide linkage analysis and evidence of gene-by-gene interactions in a sample of 362 multiplex Parkinson disease families. Hum Molec Genet. 2003; 12: 2599-608.
145) Scott WK, Nance MA, Watts RL, et al. Complete genomic screen in Parkinson disease: evidence for multiple genes. JAMA. 2001: 286; 2239-44,
146) Hutton M, Lendon CL, Rizzu P, et al. Association of missense and 5'-splice-site mutations in tau with the inherited dementia FTDP-17. Nature. 1998; 393: 702-5.
147) Baker M, Mackenzie IR, Pickering-Brown SM, et al. Mutations in progranulin cause tau-negative frontotemporal dementia linked to chromosome 17. Nature. 2006; 442: 916-9.
148) Cruts M, Gijselinck I, van der Zee J, et al. Null mutations in progranulin cause ubiquitin-positive frontotemporal dementia linked to chromosome 17q21. Nature. 2006; 442: 920-4.
149) Boeve BF, Hutton M. Refining frontotemporal dementia with parkinsonism linked to chromosome 17: introducing FTDP-17 (MAPT) and FTDP-17 (PGRN). Arch Neurol. 2008; 65: 460-4. (Review).
150) Healy DG, Abou-Sleiman PM, Lees AJ, et al. Tau gene and Parkinson's disease: a case-control study and meta-analysis. J Neurol Neurosurg Psychiatry. 2004; 75: 962-5.
151) Zabetian CP, Hutter CM, Factor SA, et al. Association analysis of MAPT H1 haplotype and subhaplotypes in Parkinson's disease. Ann Neurol. 2007; 62: 137-44.
152) Tobin JE, Latourelle JC, Lew MF, et al. Haplotypes and gene expression implicate the MAPT region for Parkinson disease: the GenePD Study. Neurology. 2008; 71: 28-34.
153) Wider C, Wszolek ZK. Rapidly progressive familial parkinsonism with central hypoventilation, depression and weight loss (Perry syndrome) —a literature review. Parkinsonism Relat. Disord. 2008; 14: 1-

7.
154) Tsuboi Y, Wszolek ZK, Kusuhara T, et al. Japanese family with parkinsonism, depression, weight loss, and central hypoventilation. Neurology. 2002; 58: 1025-30.
155) Farrer MJ, Hulihan MM, Kachergus JM, et al. DCTN1 mutations in Perry syndrome. Nat Genet. 2009; 41: 163-5.
156) LaMonte BH, Wallace KE, Holloway BA, et al. Disruption of dynein/dynactin inhibits axonal transport in motor neurons causing late-onset progressive degeneration. Neuron. 2002; 34: 715-27.
157) Vilariño-Güell C, Wider C, Soto-Ortolaza AI, et al. Characterization of DCTN1 genetic variability in neurodegeneration. Neurology. 2009; 72: 2024-8.
158) Zimran A, Neudorfer O, Elstein D. The glucocerebrosidase gene and Parkinson's disease in Ashkenazi Jews. N Engl J Med. 2005; 352: 728-31; author reply-31.
159) Aharon-Peretz J, Badarny S, Rosenbaum H, et al. Mutations in the glucocerebrosidase gene and Parkinson disease: phenotype-genotype correlation. Neurology. 2005; 65: 1460-1.
160) Gwinn-Hardy K, Chen JY, Liu HC, et al. Spinocerebellar ataxia type 2 with parkinsonism in ethnic Chinese. Neurology. 2000; 55: 800-5.
161) Payami H, Nutt J, Gancher S, et al. SCA2 may present as levodopa-responsive parkinsonism. Mov Disord. 2003; 18: 425-9.
162) Furtado S, Payami H, Lockhart PJ, et al. Profile of families with parkinsonism-predominant spinocerebellar ataxia type 2 (SCA2). Mov Disord. 2004; 19: 622-9. (Review).
163) Segawa M, Ohmi K, Itoh S, et al. Childhood basal ganglia disease with remarkable response to L-dopa, "hereditary progressive basal ganglia disease with marked diurnal fluctuation." Shinryo. 1971; 24: 667-72.
164) Segawa M, Hosaka A, Miyagawa F, et al. Hereditary progressive dystonia with marked diurnal fluctuation. Adv Neurol. 1976; 14: 215-33.
165) Ichinose H, Ohye T, Takahashi E, et al. Hereditary progressive dystonia with marked diurnal fluctuation caused by mutations in the GTP cyclohydrolase I gene. Nat Genet. 1994; 8: 236-42.
166) Segawa M, Nomura Y, Nishiyama N. Autosomal dominant guanosine triphosphate cyclohydrolase I deficiency (Segawa disease). Ann Neurol. 2003; 54 Suppl 6: S32-45. (Review).
167) Kraytsberg Y, Kudryavtseva E, McKee AC, et al. Mitochondrial DNA deletions are abundant and cause functional impairment in aged human substantia nigra neurons. Nat Genet. 2006; 38: 518-20.
168) Davidzon G, Greene P, Mancuso M, et al. Early-onset familial parkinsonism due to POLG mutations. Ann Neurol. 2006; 59: 859-62.
169) Van der Walt JM, Nicodemus KK, Martin ER, et al. Mitochondrial polymorphisms significantly reduce the risk of Parkinson disease. Am J Hum Genet. 2003; 72: 804-11.
170) Kobayashi T, Matsumine H, Matuda S, et al. Association between the gene encoding the E2 subunit of the alpha-ketoglutarate dehydrogenase complex and Parkinson's disease. Ann Neurol. 1998; 43: 120-3.
171) Latsoudis H, Spanaki C, Chlouverakis G, et al. Mitochondrial DNA polymorphisms and haplogroups in Parkinson's disease and control individuals with a similar genetic background. J Hum Genet. 2008; 53: 349-56.
172) Funayama M, Li Y, Tsoi TH, et al. Familial parkinsonism with digenic parkin and PINK1 mutations. Mov Disord. 2008: 23; 1461-5.
173) Tang B, Xiong H, Sun P, et al. Association of PINK1 and DJ-1 confers digenic inheritance of early-onset Parkinson's disease. Hum Mol Genet. 2006; 15: 1816-25.
174) Dächsel JC, Mata IF, Ross OA, et al. Digenic parkinsonism: investigation of the synergistic effects of PRKN and LRRK2. Neurosci Lett. 2006; 410: 80-4.
175) Orr-Urtreger A, Shifrin C, Rozovski U, et al. The LRRK2 G2019S mutation in Ashkenazi Jews with

Parkinson disease: is there a gender effect? Neurology. 2007; 69: 1595-602.
176) Mata IF, Samii A, Schneer SH, et al. Glucocerebrosidase gene mutations: a risk factor for Lewy body disorders. Arch Neurol. 2008; 65: 379-82.
177) Wu T, Zeng Y, Ding X, et al. A novel P755L mutation in LRRK2 gene associated with Parkinson's disease. Neuroreport. 2006; 17: 1859-62.
178) Tomiyama H, Mizuta I, Li Y, et al. LRRK2 P755L variant in sporadic Parkinson's disease. J Hum Genet. 2008; 53: 1012-5.
179) Strachan T, Read AP, 著. 村松正實, 木南 凌, 監修. Human Molecular Genetics. ヒトの分子遺伝学. 東京: メディカル・サイエンス・インターナショナル; 2003.

Journal of Human Genetics (2011) 56, 102–103

www.nature.com/jhg

COMMENTARY

A Commentary on Axon guidance pathway genes and Parkinson's disease

Hiroyuki Tomiyama

Journal of Human Genetics (2011) **56**, 102–103; doi:10.1038/jhg.2010.153; published online 2 December 2010

Axon guidance pathway is one of the critical processes related to connectivity and repair of the wiring of the brain during the central nervous system development and throughout the lifetime in humans. Indeed, many axon guidance molecules have been shown to persist in the central nervous system having roles in not only precise neuronal network formation during development but also maintenance and plasticity of neural circuits.[1]

In 1997, Livesey *et al.*[2] reported that genetic variability in the axon guidance pathway was a possible factor contributing to the development of one of the major neurodegenerative disorders, Parkinson's disease (PD), in Caucasians. In 2005, genome-wide association study by Maraganore *et al.*[3] revealed variants (single-nucleotide polymorphisms (SNPs)) in the axon guidance pathway genes related to PD susceptibility. The five mapped axon guidance pathway genes—deleted in colorectal carcinoma (*DCC*), ephrin receptor B1 (*EPHB1*), netrin-G1 (*NTNG1*), semaphorin 5A (*SEMA5A*) and *SLIT3*—were found to have SNPs associated with the prediction of PD outcomes (susceptibility, survival free of PD and age at onset of PD).[3,4] Especially, *SEMA5A* had significant association with PD, suggesting a possible role for axon guidance in the pathogenesis of PD, such as early neurodegeneration in the subclinical period and possibly even during brain development (the miswiring hypothesis).[3,4]

Functionally, the axon guidance pathway consists of four major classes of ligands (ephrin, netrin, semaphorin and slit proteins), their respective receptors (for example, eph, DCC and unc, neuropilin and plexin and robo proteins) and several downstream signaling proteins.[4] DCC-deficient adult mice showed altered dopamine transmission and locomotor activity accompanied by reduced dendritic spine density in the cerebral cortex.[5] These findings show that DCC is a crucial molecule in the development of dopamine circuitry, and alterations in *DCC* levels can lead to cognitive and behavioral abnormalities in adulthood.[4,5] In *EPHB1*-knockout mice, there is a significant cell loss in the substance nigra pars reticulata, but there is no obvious change in the number of dopamine neurons in the substance nigra pars compacta.[6] Differential expression of *NTNG1* could alter dopaminergic and glutamatergic circuitry.[4] *SEMA5A* could be involved in increasing the risk of PD by causing synaptic activity dysfunction and inflammation.[4] Concerning *SLIT3*, Slit3/robo pathway is thought to initiate and accelerate the processes or progression of PD.[4] Thus, several axon guidance pathway genes and proteins have been considered as important molecules for dopamine axonal maintenance, regeneration and target recognition.

However, some subsequent studies, including analyses on other genes, showed that the axon guidance pathway genes had no association or very weak association with PD. Although one replication study did not replicate the data, two other replication studies performed pathway-based analyses of three genome-wide association data sets of PD and concluded that axon guidance was significantly associated with PD susceptibility.[7,8] The discrepancy complicated our understandings of the role of the axon guidance pathway in PD. Although disease associations for single SNPs having small effects are difficult to replicate, the findings of the axon guidance pathway genes and the 'common disease-multiple rare variants' hypothesis suggest that the combined effects of variants within functionally related genes in certain pathways could have significant or larger effects.

In this issue, Kim *et al.*[9] investigated whether the genetic variability in the axon guidance pathway is a susceptibility factor in PD patients in the Korean population. To my knowledge, this is the first report from an Asian population about variants in the axon guidance pathway genes in PD. A set of 22 SNPs was analyzed in 373 patients and 384 healthy controls, and the risk of PD was evaluated using odds ratios in unconditional and conditional logistic regression models in age- and gender-matched subsets. Among the axon guidance pathway genes, *DCC* rs17468382 and *EPHB1* rs2030737 SNPs were found to be significantly associated with increased PD risk, and the *CHP* rs6492998 and *RRAS2* rs2970332 SNPs were found to be significantly associated with reduced PD risk. They found no association of *SEMA5A*, which was thought to have a role in the development of dopaminergic neurons and to interact with other proteins in the axon guidance pathway, with PD. Subsequent multidimensionality reduction analysis to explore potential gene–gene interactions showed that there were no significant interactions among the above-mentioned SNPs.

Although two recent large genome-wide association study studies in Japanese and Europeans have not reported the involvement of the axon guidance pathway genes in PD,[10,11] the study in the Korean population provides new data suggesting that these genes were susceptibility factors in PD patients; this made us reconsider the role of the axon guidance pathway in the pathogenesis of

Dr H Tomiyama is at the Department of Neurology, Juntendo University School of Medicine, 2-1-1 Hongo, Bunkyo, Tokyo 113-8421, Japan.
E-mail: tomiyama@juntendo.ac.jp

PD. Although no significant interactions among their SNPs in the axon guidance pathway genes were observed, investigations on interactions among other common and rare variants in the key genes of PD, such as *α-synuclein* and *LRRK2*, could be interesting. Thus, larger studies on candidate genes and SNPs or further genome-wide association study data analyses in various populations are warranted. Even if each variant has only a weak role, together added-up roles of many variants and gene–gene interaction of many genes in some common pathways could have a greater impact on the pathogenesis of multifactorial diseases such as PD.

Moreover, several lines of recent evidence support the challenging hypothesis that aberrant expression or function of axon guidance proteins such as semaphorins, ephrins, netrins and slits, which are normally involved in sculpting and maintaining motor neuron circuits, may induce pathological changes in the motor neuron circuitry and contribute to the pathogenic mechanism involved in the development of amyotrophic lateral sclerosis.[12] Furthermore, SNP models for PD were subsequently refined and compared with those of the axon guidance pathway that were highly predictive of amyotrophic lateral sclerosis susceptibility.[13]

Therefore, the axon guidance pathway SNP models could be therapeutic targets (for example, axon-regeneration therapy) for neurodegenerative disorders such as PD and amyotrophic lateral sclerosis. The genomic pathway approach might lead to new breakthroughs in the multiple disease pathways for many common, complex or overlapping disorders.

Thus, the role of axon guidance pathway should be further elucidated in common pathways for the development of PD and other neurodegenerative disorders.

CONFLICT OF INTEREST

The author declares no conflict of interest.

1 Curinga, G. & Smith, G. M. Molecular/genetic manipulation of extrinsic axon guidance factors for CNS repair and regeneration. *Exp. Neurol.* **209,** 333–342 (2008).
2 Livesey, F. J. & Hunt, S. P. Netrin and netrin receptor expression in the embryonic mammalian nervous system suggests roles in retinal, striatal, nigral, and cerebellar development. *Mol. Cell Neurosci.* **8,** 417–429 (1997).
3 Maraganore, D. M., de Andrade, M., Lesnick, T. G., Strain, K. J., Farrer, M. J., Rocca, W. A. *et al.* High-resolution whole-genome association study of Parkinson disease. *Am. J. Hum. Genet.* **77,** 685–693 (2005).
4 Lin, L., Lesnick, T. G., Maraganore, D. M. & Isacson, O. Axon guidance and synaptic maintenance: preclinical markers for neurodegenerative disease and therapeutics. *Trends. Neurosci.* **32,** 142–149 (2009).
5 Grant, A., Hoops, D., Labelle-Dumais, C., Prévost, M., Rajabi, H., Kolb, B. *et al.* Netrin-1 receptor-deficient mice show enhanced mesocortical dopamine transmission and blunted behavioural responses to amphetamine. *Eur. J. Neurosci.* **26,** 3215–3228 (2007).
6 Richards, A. B., Scheel, T. A., Wang, K., Henkemeyer, M. & Kromer, L. F. EphB1 null mice exhibit neuronal loss in substantia nigra pars reticulata and spontaneous locomotor hyperactivity. *Eur. J. Neurosci.* **25,** 2619–2628 (2007).
7 Wang, K., Li, M. & Bucan, M. Pathway-based approaches for analysis of genomewide association studies. *Am. J. Hum. Genet.* **81,** 1278–1283 (2007).
8 Srinivasan, B. S., Doostzadeh, J., Absalan, F., Mohandessi, S., Jalili, R., Bigdeli, S. *et al.* Whole genome survey of coding SNPs reveals a reproducible pathway determinant of Parkinson disease. *Hum. Mutat.* **30,** 228–238 (2008).
9 Kim, J.- M., Park, S. K., Yang, J. J., Shin, E.- S., Lee, J.- Y., Yun, J. Y. *et al.* SNPs in axon guidance pathway genes and susceptibility for Parkinson's disease in the Korean population. *J. Hum. Genet.* **56,** 125–129 (2011).
10 Satake, W., Nakabayashi, Y., Mizuta, I., Hirota, Y., Ito, C., Kubo, M. *et al.* Genome-wide association study identifies common variants at four loci as genetic risk factors for Parkinson's disease. *Nat. Genet.* **41,** 1303–1307 (2009).
11 Simón-Sánchez, J., Schulte, C., Bras, J. M., Sharma, M., Gibbs, J. R., Berg, D. *et al.* Genome-wide association study reveals genetic risk underlying Parkinson's disease. *Nat. Genet.* **41,** 1308–1312 (2009).
12 Schmidt, E. R., Pasterkamp, R. J. & van den Berg, L. H. Axon guidance proteins: novel therapeutic targets for ALS? *Prog. Neurobiol.* **88,** 286–301 (2009).
13 Lesnick, T. G., Sorenson, E. J., Ahlskog, J. E., Henley, J. R., Shehadeh, L., Papapetropoulos, S. *et al.* Beyond Parkinson disease: amyotrophic lateral sclerosis and the axon guidance pathway. *PLoS One* **3,** e1449 (2008).

Autophagy 7:2, 176-187; February 2011; © 2011 Landes Bioscience

Caffeine induces apoptosis by enhancement of autophagy via PI3K/Akt/mTOR/p70S6K inhibition

Shinji Saiki,[1] Yukiko Sasazawa,[2] Yoko Imamichi,[1] Sumihiro Kawajiri,[1] Takahiro Fujimaki,[2] Isei Tanida,[3] Hiroki Kobayashi,[2] Fumiaki Sato,[4] Shigeto Sato,[1] Kei-Ichi Ishikawa,[1] Masaya Imoto[2] and Nobutaka Hattori[1,*]

[1]Department of Neurology; Juntendo University School of Medicine; Bunkyo, Tokyo; [2]Department of Biosciences and Informatics; Faculty of Science and Technology; Keio University; Kohoku, Yokohama; [3]Department of Biochemistry and Cell Biology; National Institute of Infectious Diseases; Shinjyuku, Tokyo; [4]Research Institute for Disease of Old Age; Juntendo University School of Medicine; Tokyo, Japan

Key words: apoptosis, autophagy, PI3K/Akt/mTOR/p70S6K, ERK1/2, caffeine

Abbreviations: PI3K, phosphoinositide-3 kinase; 4E-BP1, eukaryotic initiation factor 4-binding protein 1; ERK, extracellular signal-regulated kinase; mTOR, mammalian target of rapamycin; 3-MA, 3-methyladenine; MEFs, mouse embryonic fibroblasts; p70S6K, 70-kDa ribosomal protein S6 kinase; PI, propidium iodide; MPP^+, 1-methyl-4-phenylpyridinium

Caffeine is one of the most frequently ingested neuroactive compounds. All known mechanisms of apoptosis induced by caffeine act through cell cycle modulation or p53 induction. It is currently unknown whether caffeine-induced apoptosis is associated with other cell death mechanisms, such as autophagy. Herein we show that caffeine increases both the levels of microtubule-associated protein 1 light chain 3-II and the number of autophagosomes, through the use of western blotting, electron microscopy and immunocytochemistry techniques. Phosphorylated p70 ribosomal protein S6 kinase (Thr389), S6 ribosomal protein (Ser235/236), 4E-BP1 (Thr37/46) and Akt (Ser473) were significantly decreased by caffeine. In contrast, ERK1/2 (Thr202/204) was increased by caffeine, suggesting an inhibition of the Akt/mTOR/p70S6K pathway and activation of the ERK1/2 pathway. Although insulin treatment phosphorylated Akt (Ser473) and led to autophagy suppression, the effect of insulin treatment was completely abolished by caffeine addition. Caffeine-induced autophagy was not completely blocked by inhibition of ERK1/2 by U0126. Caffeine induced reduction of mitochondrial membrane potentials and apoptosis in a dose-dependent manner, which was further attenuated by the inhibition of autophagy with 3-methyladenine or *Atg7* siRNA knockdown. Furthermore, there was a reduced number of early apoptotic cells (annexin V positive, propidium iodide negative) among autophagy-deficient mouse embryonic fibroblasts treated with caffeine than in their wild-type counterparts. These results support previous studies on the use of caffeine in the treatment of human tumors and indicate a potential new target in the regulation of apoptosis.

Introduction

Caffeine has a diverse range of pharmacological effects.[1] In addition to its various effects on the cell cycle and growth arrest, higher (4–10 mM) concentrations of caffeine can induce apoptosis in several cell lines, such as 10 mM caffeine in human neuroblastoma cells,[2] 4 mM caffeine in human pancreatic adenocarcinoma cells[3] and 5 mM caffeine in human A549 lung adenocarcinoma cells.[4] Although caffeine has been reported to modulate cell cycle checkpoints and perturb molecular targets of the cell cycle, the exact mechanism of caffeine-induced apoptosis remains unclear.[1]

Autophagy is a key mechanism in various physiopathological processes, including tumorigenesis, development, cell death and survival.[5,6] It has also been shown to have a complex relationship with apoptosis, especially in tumor cell lines.[7] Several reports have shown that autophagy not only enhances caspase-dependent cell death, but is also required for it.[8] In contrast, it has also been shown that autophagy plays an important role in promoting cell survival against apoptosis.[7] Caffeine has been reported to inhibit some kinase activities, including various forms of phosphoinositol-3 kinase and mammalian target of rapamycin (mTOR).[9,10] Recently, in food spoilage studies involving yeast, caffeine has been shown to induce a starvation response,[11] which is a key regulator of autophagy causing its induction. However, the exact mechanism by which caffeine induces autophagy is still unknown.

Here we report that higher concentrations of caffeine enhance autophagic flux in a dose-dependent manner in various cell lines. Furthermore, we show that caffeine-induced autophagy is mainly dependent on PI3K/Akt/mTOR/p70S6 signaling and eventually results in apoptosis.

*Correspondence to: Nobutaka Hattori; Email: nhattori@juntendo.ac.jp
Submitted: 06/22/10; Revised: 10/27/10; Accepted: 11/02/10
Previously published online: www.landesbioscience.com/journals/autophagy/article/14074
DOI: 10.4161/auto.7.2.14074

Results and Discussion

Caffeine (**Fig. 1A**) is a widely used psychoactive drug that has been used for centuries to increase alertness and energy. It has been reported that caffeine induces autophagy in *Zygosaccharomyces bailii* in association with a starvation response, caused by a unknown mechanism.[11] However, it remains unknown whether caffeine affects autophagy in mammalian cells. To determine if caffeine regulates autophagy at a steady state, we first examined levels of the microtubule-associated protein 1 light chain 3 (LC3)-II, which is an LC3-phosphatidyl-ethanolamine conjugate and a promising autophagosomal marker.[12] LC3-II levels (compared to actin loading controls) increased with 5–25 mM caffeine treatment over 48 hours in SH-SY5Y (**Fig. 1B and C**), PC12D and HeLa cells (**Suppl. Fig. S1A and B**). The LC3-II/actin ratio also increased in a time-dependent manner in SH-SY5Y (**Fig. 1D and E**) and HeLa cells (data not shown). Using an electron microscopy technique, the numbers of autophagic vacuoles (AVs) were markedly increased in SH-SY5Y cells treated with 10 or 25 mM caffeine, but not in the control (**Fig. 1F and G**). Morphometric analysis revealed that the number of AVs per 100 μm^2 of SH-SY5Y cytoplasm in control (Mean ± standard deviation: 1.3 ± 0.50), whereas that in caffeine-treated cells (10 mM: 8.0 ± 0.82; 25 mM: 15 ± 1.9) for 24 hours. Expression levels of p62, a well-known autophagic substrate, were also decreased by caffeine treatment in SH-SY5Y (**Fig. 1H and I**) and HeLa cells (**Suppl. Fig. S1C and D**). Furthermore, 10 mM caffeine treatment markedly increased the number of EGFP-LC3-positive vesicles in SH-SY5Y cells transiently transfected with EGFP-LC3 (data not shown) and HeLa cells stably expressing EGFP-LC3 (**Figs. 1J and K**).[12,13] This effect was confirmed by the observation that caffeine administration also increased the number of vesicles positive to endogenous LC3 (**Suppl. Fig. S1E**).

Endogenous LC3 is post-transcriptionally processed into LC3-I, which is found in the cytosol. LC3-I is in turn lipidated to LC3-II, which then associates with autophagosome membranes.[14] LC3-II can accumulate due to increased upstream autophagosome formation or impaired downstream autophagosome-lysosome fusion. To distinguish between these two possibilities, we assayed LC3-II in the presence of E64D plus pepstatin A or bafilomycin A1, which inhibits lysosomal proteases or blocks downstream autophagosome-lysosome fusion and lysosomal proteases, respectively.[15,16] Caffeine significantly increased LC3-II levels in the presence of E64d plus pepstatin A or bafilomycin compared to E64d plus pepstatin A or bafilomycin alone in (**Fig. 2A and B**; **Suppl. Fig. S1F and G**) and HeLa cells (**Fig. 2C and D**; **Suppl. Fig. S1H and I**). A saturating dosage of bafilomycin A1 was used in this assay and no further increases in LC3-II levels were observed when cells were treated with higher concentrations. Similar results were observed in PC12D cell lines (data not shown). To confirm the caffeine effect on autophagic flux, we assessed the numbers of autolysosomes and autophagosomes in HeLa cells. The ratio of the numbers of autolysosomes (positive to both LC3 and LAMP2) to autophagosomes (positive to LC3) was increased by 10 mM caffeine treatment for 48 hours (**Fig. 2E**). Quantification data using ImageJ also showed significant increase of the ratio (**Fig. 2F**). These results strongly indicate that high concentration of caffeine treatment enhances autophagic flux.

The class I phosphatidylinositol 3-phosphate kinase (PI3K)/Akt/mTOR/p70ribosomal protein S6 kinase (p70S6K) signaling pathway and the Ras/Raf-1/mitogen-activated protein kinase 1/2 (MEK1/2)/extracellular signal-regulated kinase 1/2 (ERK1/2) pathway are two well-known pathways involved in the regulation of autophagy. Both are associated with tumorigenesis and often activated in numerous types of tumors.[17] Therefore, we examined the effect of caffeine on both of these pathways, using western blotting, according to the protocol by Inoki and colleagues.[18] After a 24 hour treatment with caffeine, there was a significant decrease in the levels of phosphorylated p70 S6 kinase, S6 ribosomal protein and 4E-BP1, compared with total normal levels in SH-SY5Y (**Fig. 3A**), HeLa and PC12D cells (data not shown). Consistent with these results, nonphosphorylated 4E-BP1 proteins were increased by caffeine treatment (**Fig. 3A**). To further investigate the upstream inhibition of mTOR by caffeine, we examined Ser473 phosphorylation of Akt, which measures both Akt/mTOR and mTORC2 activity. As shown in **Figure 3B**, treatment with caffeine also decreased the level of phosphorylated Akt in SH-SY5Y cells, which was consistent with a previous report.[19] Similar findings were obtained in HeLa (**Suppl. Fig. S2A**) and PC12D cells (data not shown). Subsequently, we examined whether caffeine increases the phosphorylation of ERK1/2, a key regulator of autophagy downstream of Akt. As shown in **Figure 3C**, treatment with caffeine increased phosphorylated ERK1/2. The effects of caffeine on mTOR inhibition were initially detected 3 hours after the addition of caffeine and reached a maximal level after 6 hours in SH-SY5Y (**Fig. 3D**) and 9 hours in HeLa cells (**Suppl. Fig. S2B and C**).

Caffeine has been shown to inhibit PI3K and components of the PI3K/Akt pathway.[9,20] Next, we performed experiments to confirm whether caffeine-induced autophagy is activated through the PI3K/Akt pathway. Insulin or insulin-like growth factor upregulates PI3K and its downstream targets including Akt and mTOR, resulting in the inactivation of autophagy.[21-23] As shown in **Figure 4A and B**, insulin treatment for 30 minutes significantly phosphorylated Akt at Ser473, whereas the phosphorylation was completely abolished by additional treatment with caffeine. No significant differences of the LC3-II/actin ratio between caffeine treatment and caffeine treatment with insulin were observed. Also, caffeine and Akt1/2 inhibitors did not have additive effects on the levels of LC3-II/actin ratio compared to the single treatment of caffeine or Akt inhibitors (**Fig. 4C and D**). To further confirm the caffeine effects on this pathway, cells were transiently transfected with myristoylated Akt (myr-Akt), a constitutively active form of Akt.[24] Caffeine treatment of both cells transfected with control vector and myr-Akt markedly decreased the levels of the phosphorylated Akt (**Fig. 3E**), indicating that caffeine directly inhibits the Akt phosphorylation. If caffeine facilitates autophagy through PI3K/Akt and ERK1/2 signalings, the autophagy should be partially blocked by ERK1/2 inhibition using the mitogen-activated protein kinase kinase 1/2 (MEK1/2) inhibitor, U0126. U0126

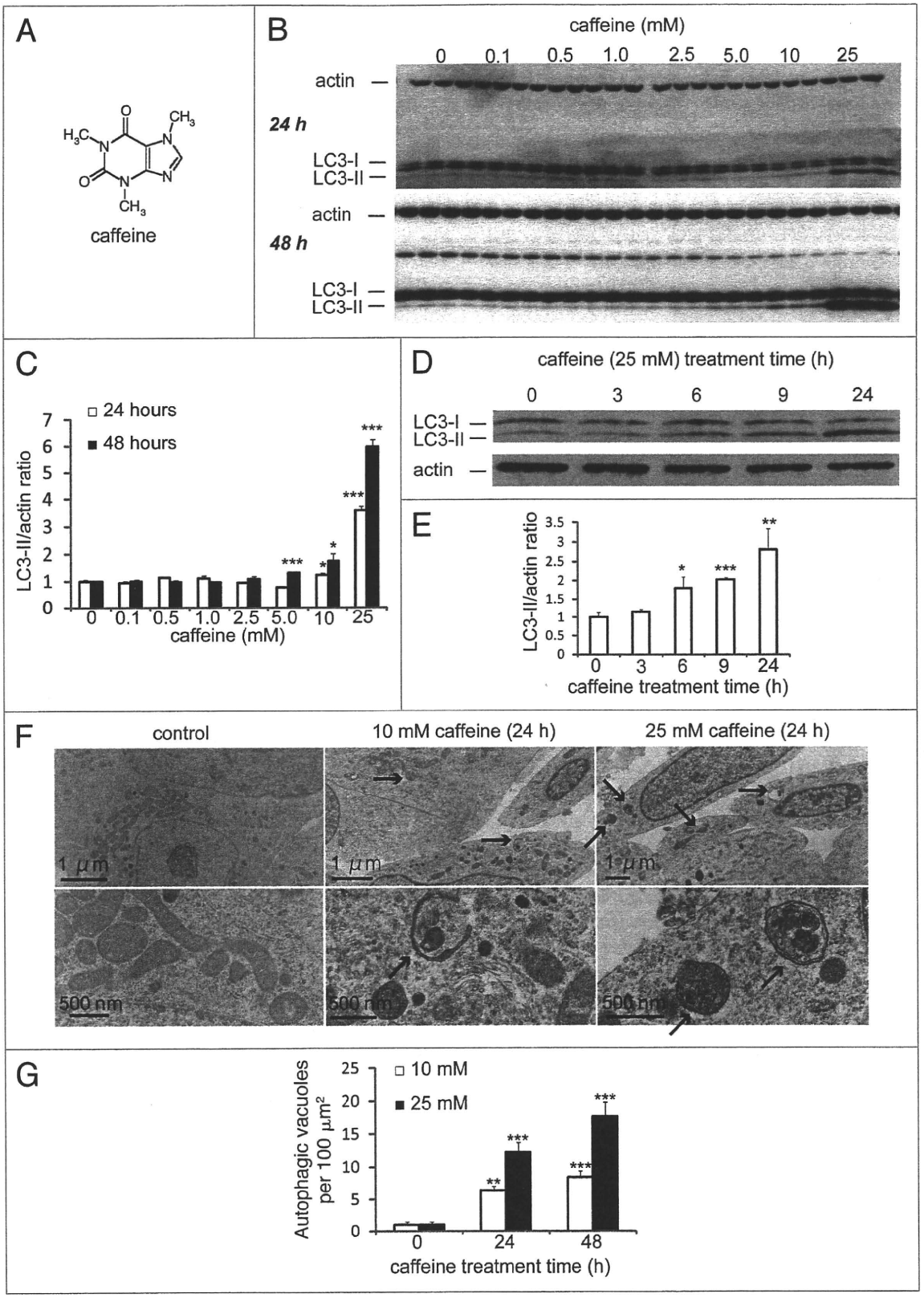

Figure 1A–G. For figure legend, see page 179.

Figure 1A–G (See opposite page). Caffeine increases autophagic flux in various cell lines. (A) Structural formula of caffeine. (B and C) SH-SY5Y cells treated with various concentrations of caffeine for 24 or 48 hours were analyzed by immunoblotting (B) with antibodies against LC3 and actin. Densitometry analysis of LC3-II levels relative to actin (C) was performed using three independent experiments. (D and E) SH-SY5Y cells treated with 25 mM caffeine for 3–24 hours were analyzed by immunoblotting (D) with antibodies against LC3 and actin. Densitometry analysis of LC3-II levels relative to actin (E) was performed using three independent experiments. (F) Electron microscopic examination of SH-SY5Y cells treated with various concentrations of caffeine for 24 or 48 hours. Autophagic vacuoles accumulating in the cytoplasm are shown by arrows. (G) Morphometric analysis of autophagic vacuoles was performed with 30 different areas of the cytoplasm of control and caffeine-treated cells.

significantly but mildly reversed the levels of LC3-II/actin ratio (**Fig. 4F and G**). The failure of U1026 to reverse completely the caffeine effect can be explained by the autophagy induction through Akt/mTOR signaling. In addition, only Akt knockdown with inducible short hairpin RNAs (shRNAs) to specifically and stably knock down all three Akt isoforms sufficiently increases autophagic flux.[25] Therefore, we concluded that the caffeine-induced autophagy is mainly dependent on the PI3K/Akt/mTOR pathway.

Because caffeine induces autophagy dependently of mTOR inhibition, we hypothesized that combination treatment of caffeine with rapamycin would not have additive effects on autophagy. However, caffeine and rapamycin showed an additive effect on the enhancement of LC3-II/actin ratio compared to the single treatment of caffeine or rapamycin (**Fig. 5A and B**). Several lines of evidences support the hypothesis that resistance to rapamycin results from a positive feedback loop from mTOR/S6K1 to Akt, resulting in enhancement of Akt phosphorylation at Ser 473.[26-28] Recently, mutual suppression of the PI3K/Akt/mTOR pathway by combination of rapamycin with perifosine, an Akt inhibitor, induces synergistic effects on autophagy-induced apoptosis as well as enhancement of autophagy, suggesting that dual inhibition of the PI3K/Akt/mTOR by rapamycin with caffeine would be also a rational treatment for cancer.[29]

Several anti-cancer agents are known to inhibit the PI3K/Akt/mTOR/p70S6K pathway and simultaneously activate ERK1/2, resulting in induction of autophagy in tumor cell lines.[30,31] The upregulation of this process has beneficial effects in neurodegenerative diseases, such as Parkinson and Huntington diseases, whereas an excess of autophagy can lead to cell death.[32,33] Therefore, we decided to investigate whether caffeine-induced autophagy rescues or induces cell death. Using PC12D cells treated with 1-methyl-4-phenylpyridinium (MPP^+), a well-established Parkinson disease model,[34] we determined that 1 mM caffeine treatment was not sufficient for the induction of autophagy (**Suppl. Fig. S4 and B**) and promoted increased cell viability, whereas >2.5 mM caffeine decreased cell viability (**Fig. 6A**). In addition, a significant decrease in cell viability was noted in cells treated with >2.5 mM caffeine without MPP^+. Also, mitochondrial membrane potentials assessed by JC-1 were significantly preserved by 1 mM caffeine treatment compared to the control with MPP^+, while those were lost by >5 mM caffeine treatment

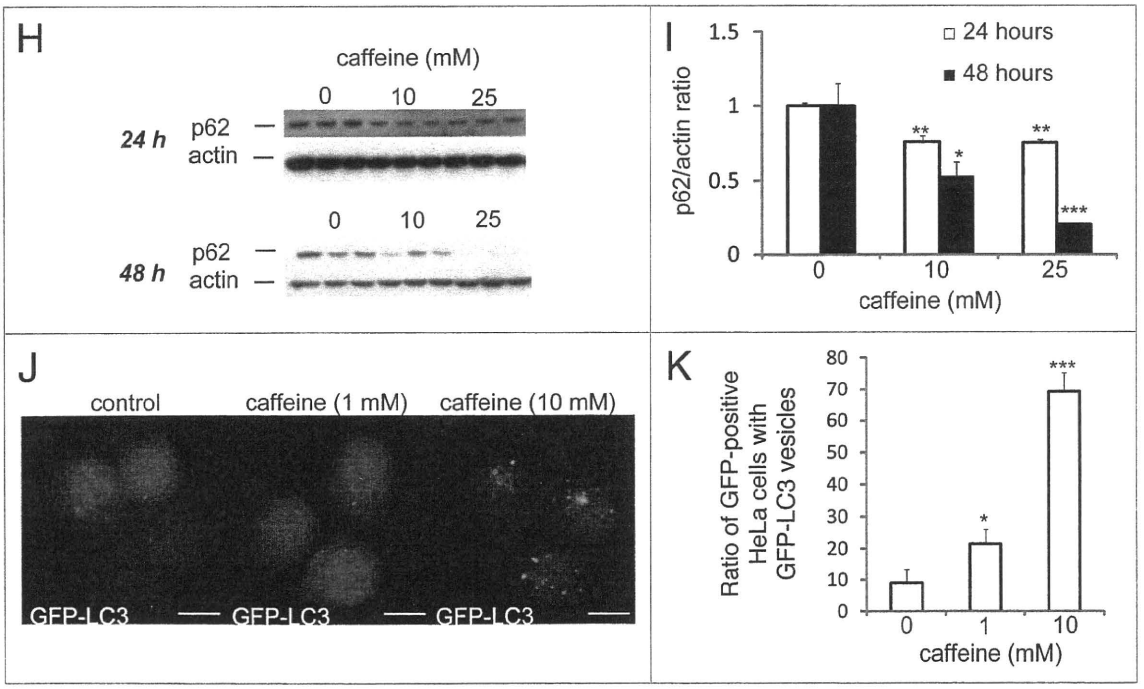

Figure 1H–K. Caffeine increases autophagic flux in various cell lines. (H and I) SH-SY5Y cells treated with various concentrations of caffeine for 24 or 48 hours were analyzed by immunoblotting with antibodies against p62 and actin. Densitometry analysis of p62 levels relative to actin (I) was performed using three independent experiments. (J and K) HeLa cells stably expressing EGFP-LC3 were treated with various concentrations of caffeine for 24 hours and analyzed using confocal microscopy. The percentage of EGFP-positive HeLa cells with >5 EGFP-LC3 vesicles was assessed (K) described previously in reference 43. Error bars, S.D.; *$p < 0.05$; **$p < 0.01$.

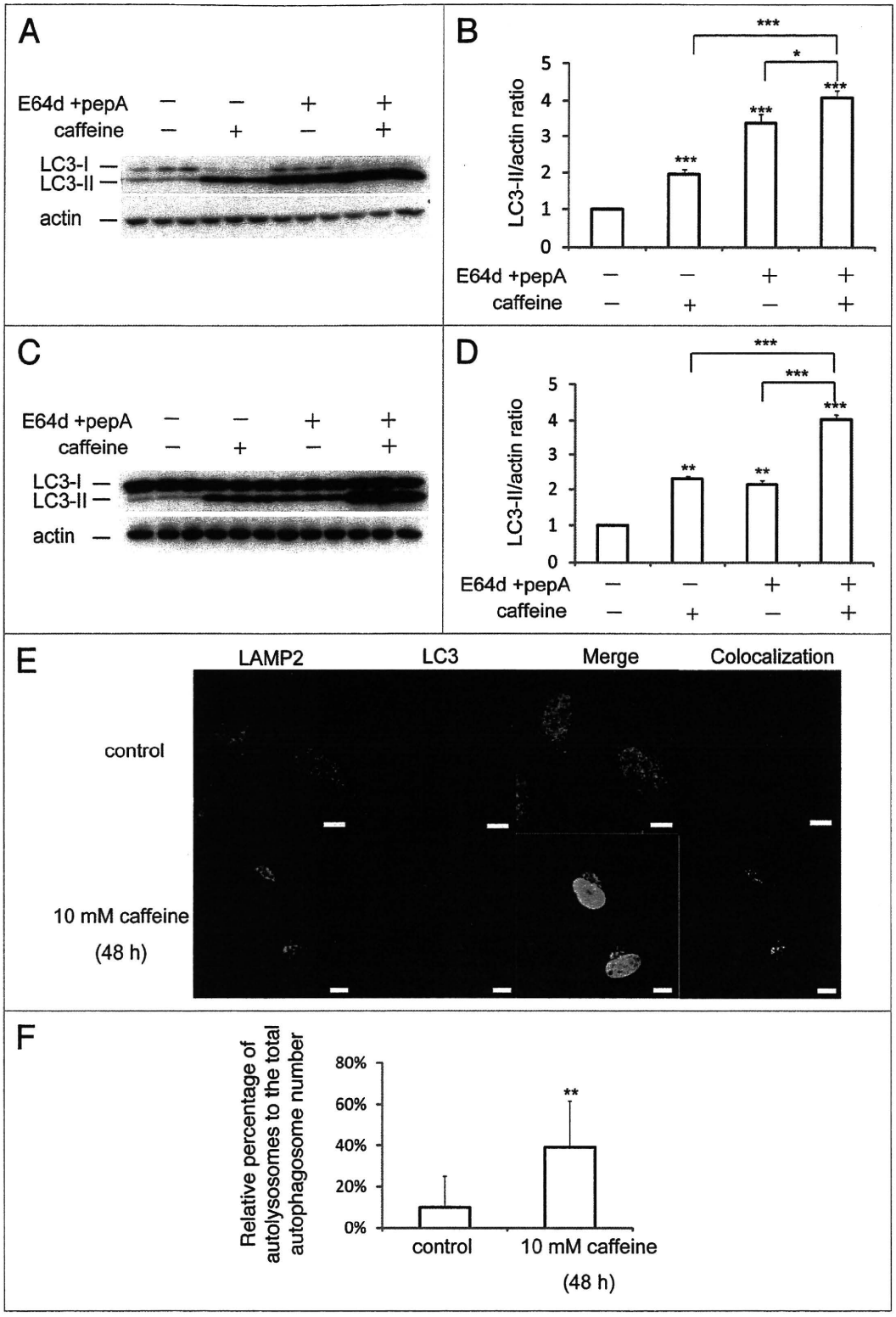

Figure 2. Caffeine does not block autophagosome-lysosome fusion. (A–D) SH-SY5Y (A) or HeLa (C) cells treated with 10 mM caffeine with or without E64d (10 μg/ml) and pepstatin A (10 μg/ml) were analyzed by immunoblotting with antibodies against LC3 and actin. Densitometry analysis of LC3 levels relative to actin in SH-SY5Y (B) and HeLa (D) cells was performed using three independent experiments. (E and F) HeLa cells treated with various concentrations of caffeine for 48 hours were analyzed using confocal microscopy (E). Number of the autolysosomes and autophagosomes were automatically counted using ImageJ "Colocalization" Plugin and the ratios were calculated (F).

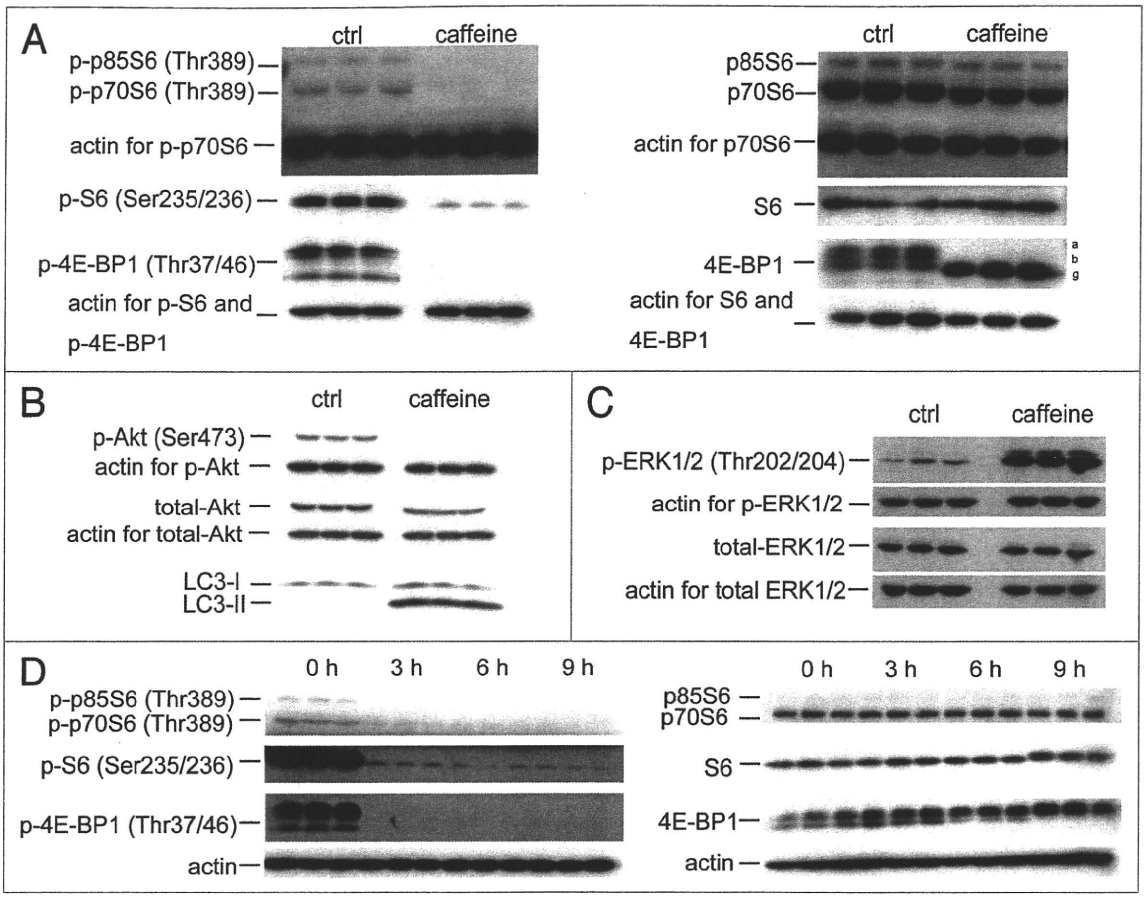

Figure 3. Caffeine inhibits the Akt/mTOR/p70S6 signaling pathway and activates ERK1/2 signaling. (A and B) SH-SY5Y cells treated with or without 10 mM caffeine for 24 hours were analyzed for mTOR activity by immunoblotting for levels of phosphor- and total p70 ribosomal S6 protein, S6, 4E-BP1 (A), Akt (B) and actin. (C) SH-SY5Y cells treated with or without 10 mM caffeine for 0, 3, 6 or 9 hours were analyzed by immunoblotting for levels of phosphor- and total ERK1/2 and actin. (D) SH-SY5Y cells treated with 10 mM caffeine for various time periods were analyzed by immunoblotting for levels of phosphor- and total p70 ribosomal S6 protein, S6, 4E-BP1 and actin.

(**Fig. 6B and Suppl. Fig. S5A**). These data suggest that caffeine-induced autophagy is not protective in these cell lines and leads to cell death.

Autophagy and apoptosis may act independently in parallel pathways or may influence one another.[7] To confirm the relationship between these pathways in cells treated with caffeine, we examined caffeine effects on the cell cycle with a propidium iodide (PI) staining assay. Treatment with 2.5–10 mM caffeine increased the percentage of cells in the sub-G_1 peak, which is indicative of apoptosis (**Fig. 6C**). To confirm whether caffeine-induced cell death is apoptotic, we examined the activity of caspase-3, a well-known inducer of apoptosis. Treatment with 10 mM caffeine markedly increased levels of cleaved caspase-3 and decreased full-length caspase-3 in PC12D cells (**Fig. 6D**), consistent with previous reports on the induction of apoptosis by caffeine.[35-37]

To test whether caffeine-induced apoptosis is dependent on autophagy, we determined whether the inhibition of autophagy by 3-methyladenine (3-MA) or Atg7 siRNA knockdown affects caffeine-induced cytotoxicity in PC12D cells. Treatment with 1 or 5 mM 3MA or Atg7 knockdown significantly decreased the percentage of cell death or cells with reduced mitochondrial membrane potentials caused by caffeine treatment (5 or 10 mM) (**Fig. 6E and F and Suppl. Fig. S6B**). As can be seen from the increased caffeine-induced apoptosis shown in **Figure 6A and C**, our data suggests that caffeine-induced autophagy is necessary for apoptotic cell death. To further confirm this, we compared autophagy-deficient mouse embryonic fibroblasts (MEFs), lacking the *Atg7* gene ($Atg7^{-/-}$), without LC3-II expression (**Suppl. Fig. S4E**), and matched wild-type ($Atg7^{+/+}$) MEFs, in which autophagy is induced by caffeine in a dose-dependent manner (**Suppl. Fig. S4C and D**). As expected, the level of caffeine-induced cell death (positive to trypan blue staining) in $Atg7^{-/-}$ MEFs was less than that in $Atg7^{+/+}$ MEFs (**Fig. 7A**). The numbers of early apoptotic cells (annexin V positive, PI negative) were significantly increased in both a time-dependent and dose-dependent manner by caffeine treatment of $Atg7^{+/+}$ MEFs compared to $Atg7^{-/-}$ MEFs (**Fig. 7B–D**). Also, apoptotic or necrotic cells (annexin V positive) were significantly increased by caffeine treatment of $Atg7^{+/+}$ MEFs compared to $Atg7^{-/-}$ MEFs (**Suppl. Fig. S6**). Together, these results indicate that caffeine-induced autophagy partly occurs upstream of apoptosis and is not a protective response to caffeine.

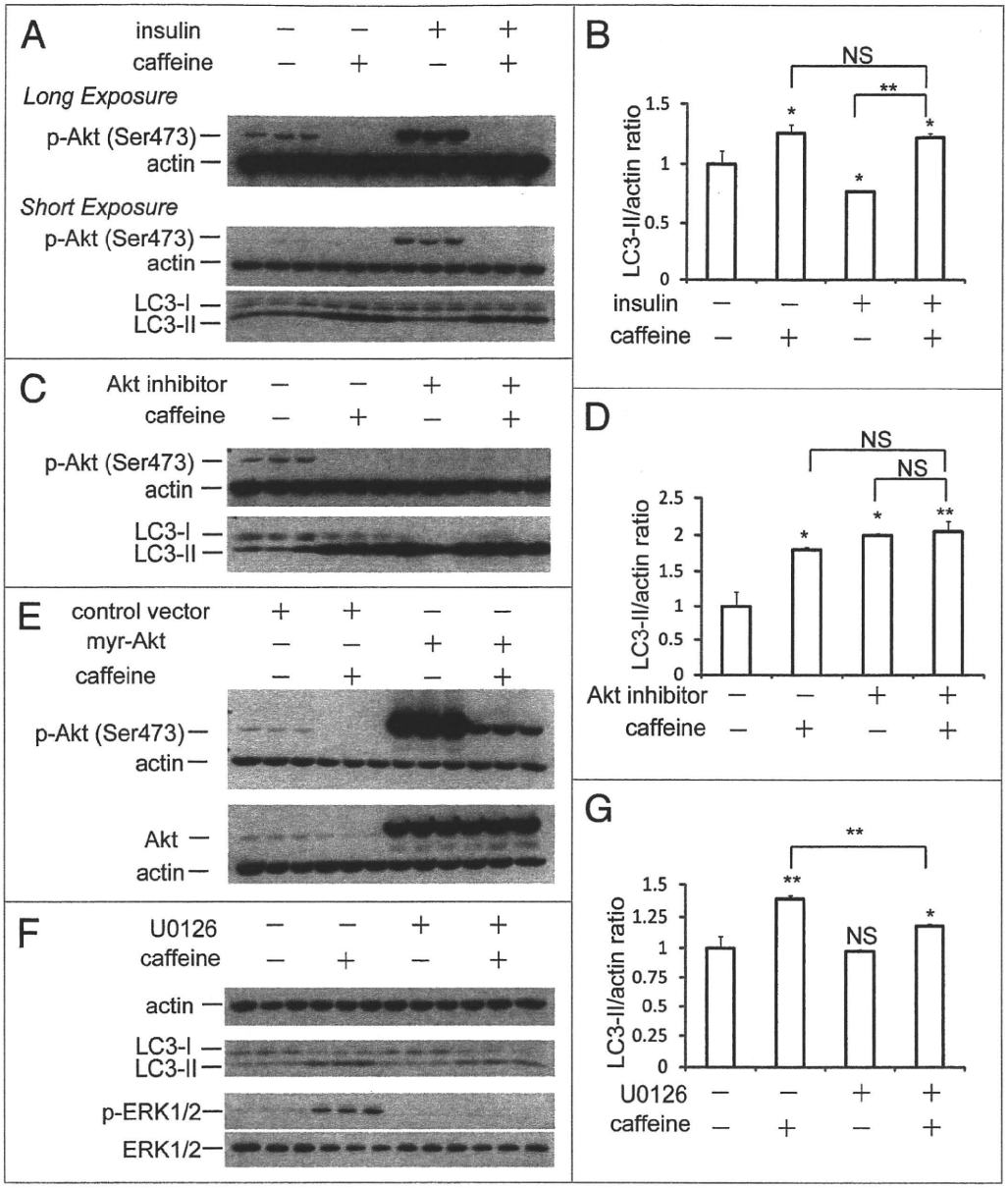

Figure 4. Caffeine-induced autophagy is dependent on PI3K/Akt/mTOR pathway. (A) SH-SY5Y cells treated with 25 mM caffeine for 3 hours followed by treatment with or without 200 nM insulin for 30 minutes were analyzed by immunoblotting. (B) Densitometry analysis of LC3-II levels relative to actin was performed using three independent experiments. (C) SH-SY5Y cells treated with 25 mM caffeine, 50 μM Akt1/2 inhibitors or 25 mM caffeine with 50 μM Akt1/2 inhibitors for 6 hours were analyzed by immunoblotting. (D) Densitometry analysis of LC3-II levels relative to actin was performed using three independent experiments. (E) SH-SY5Y cells were transfected for 24 hours with either a control plasmid DNA (pcDNA3.1) or a plasmid encoding constitutively active Akt (myr-Akt), and then treated with H_2O or 10 mM caffeine for 6 hours. Immunoblotting was performed using antibodies against Akt, p-Akt (Ser 473) and actin. (F) SH-SY5Y cells treated with 25 mM caffeine with or without 20 μM U0126 for 6 hours were analyzed by immunoblotting using antibodies against actin, LC3, p-ERK and ERK. (G) Densitometry analysis was performed using three independent experiments. Error bars, SD; *$p < 0.05$; **$p < 0.01$; N.S., not significant.

In various tumor cell lines, higher concentrations of caffeine alone induce p53-dependent G_1 phase arrest and under certain conditions apoptosis can also occur in a p53-independent manner.[1] Furthermore, disruption at the G_2/M checkpoint by caffeine allows cells time to repair DNA damage by driving them through mitosis, eventually resulting in apoptosis.[36,38,39] Consistent with these reports, the results of our study indicate that increased concentrations of caffeine treatment cause a dose-dependent increase in apoptosis. More recently, autophagy, a process long known to provide a survival advantage to cells undergoing nutrient deprivation and other stresses, has also been linked to the cell death process.[7] The cross-talk between apoptosis and autophagy is complex and sometimes contradictory; however, it is critical to the overall fate of the cell. In this study, we have shown that autophagy is induced by higher concentrations of caffeine without starvation, mainly via the inhibition of PI3K/Akt/mTOR/p70S6K signaling.

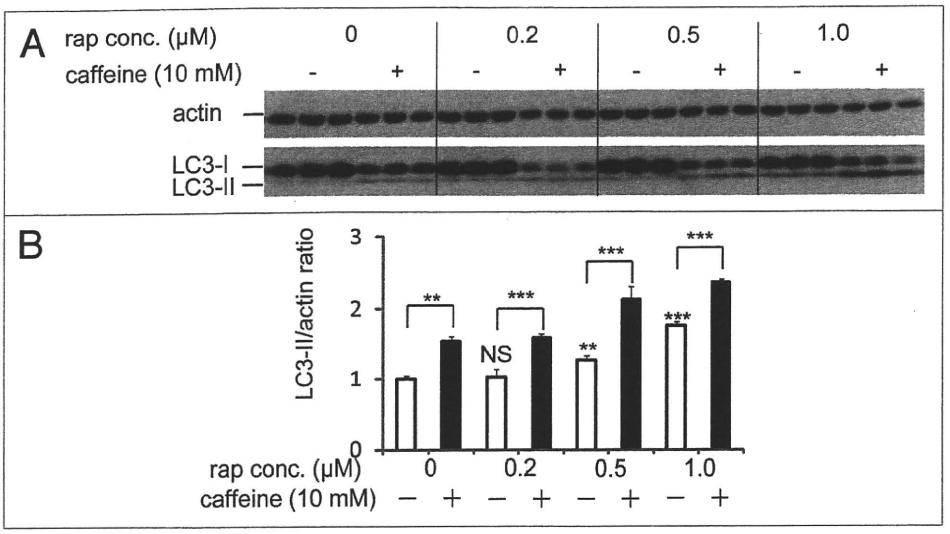

Figure 5. Rapamycin treatment with caffeine has an additive effect on enhancement of autophagy. (A) SH-SY5Y cells treated with various concentrations of rapamycin with or without 10 mM caffeine for 48 hours were analyzed by immunoblotting. (B) Densitometry analysis was performed using three independent experiments. Error bars, SD; *p < 0.05; **p < 0.01; N.S., not significant.

Likewise, when caffeine-induced autophagy is blocked by 3-MA treatment or *Atg7* knockout, apoptosis is partially attenuated, suggesting that caffeine-induced autophagy occurs upstream of caffeine-induced apoptosis. It also indicates the involvement of other pathways in caffeine-induced apoptosis. These results provide new insight into the effects of caffeine on cell death and survival and its use as a possible intervention strategy for the upregulation of apoptosis by a harnessing of its autophagic activity in tumor treatment.

Materials and Methods

Cell line. HeLa cells were maintained in DMEM (Sigma) supplemented with 10% fetal bovine serum (FBS) (Sigma) and 100 U/ml penicillin/streptomycin (Sigma) at 37°C and 5% CO_2. PC12D and SH-SY5Y cells were maintained in DMEM (Sigma) supplemented with 10% FBS (Sigma), 5% horse serum and 100 U/ml penicillin/streptomycin at 37°C and 5% CO_2. All experiments with PC12D were performed after differentiation with NGF treatment for 48 hours. *Atg7*$^{+/+}$ and $^{-/-}$ MEFs were maintained in DMEM (Sigma) supplemented with 10% FBS, 100 U/ml penicillin/streptomycin, 1% sodium pyruvate (Gibco, 11360), 1% non-essential amino acid (NEAA) and 4.2 μl 2% beta-mercaptoethanol at 37°C.

To establish a HeLa GFP-LC3 stable cell line, proliferating HeLa cells were transfected with a GFP-LC3 plasmid.[14] Forty-eight hours post-transfection with Lipofectamine 2000 (Invitrogen), positive stable clones were selected by growing cells with G418 (400 μg/ml) for 2 weeks and maintained in DMEM (Sigma) supplemented with 10% FBS (Sigma), 100 U/ml penicillin/streptomycin and 200 μg/ml G418 at 37°C and 5% CO_2. All cellular experiments were performed with cells cultured in complete medium with FBS as explained above.

Cell viability assays. A trypan blue dye (Invitrogen, 15250-061) exclusion assay was used to examine cell viability and performed according to previously reported protocols.[40,41] Changes of mitochondrial membrane potentials were assessed also with the lipophilic cationic membrane potential-sensitive dye JC-1 (5,5',6,6'-tetrachloro-1,1',3,3'-tetraehylbenzimidazolylcarbocyanineiodide) (Wako, 106-00131) according to the manufacturer's protocol. Detection of early apoptotic cells was determined using an annexin V/propidium iodide (PI) detection kit (Invitrogen), according to the manufacturer's protocol. Briefly, 0.5 x 10^6 *Atg7*$^{+/+}$ or $^{-/-}$ MEFs were exposed to caffeine (0–25 mM) for 24 hours and washed twice. Then, they were incubated at room temperature with annexin V/Alexa488 and PI for 15 minutes. Annexin V$^+$PI$^-$ cells, considered as early apoptotic cells, were enumerated using FACScan (BD Biosciences). Data were analyzed with CellQuest (BD Biosciences) and FlowJo softwares (Tree Star Inc.). Cells positive or negative for annexin V were regarded as apoptotic or non-apoptotic cells, respectively.

Cell cycle analysis. To examine apoptosis, 1.0 x 10^4 cells/well PC12D cells were seeded onto 96-well culture plate and incubated for 48 h in DMEM with NGF and treated with caffeine for 72 h. The cells were harvested and washed with PBS and fixed with ice-cold 70% ethanol at 4°C for 2 h. The cells were then stained with PI solution according to previously reported protocol.[41] DNA content was analyzed by

Figure 6 (See next page). Caffeine induces apoptosis by enhancement of autophagy. (A) After PC12D cells were treated with 0, 1, 2.5, 5 or 10 mM caffeine with DMSO or MPP$^+$ for 72 hours, cell viability was measured using trypan blue dye exclusion assay. Data are the means of triplicate experiments. (B) After cells were treated with 0, 1, 2.5, 5 or 10 mM caffeine with DMSO or MPP$^+$ for 48 hours, mitochondrial membrane potential was analyzed by JC-1 using a flow cytometry. Data are the means of triplicate experiments. (C) After PC12D cells were treated with 0, 1, 2.5, 5 or 10 mM caffeine with DMSO or MPP$^+$ for 72 hours, caffeine-induced sub G_1 area was analyzed by propidium iodide staining assay using a flow cytometry. Data are the means of triplicate experiments. (D) PC12D cells were treated with H_2O or caffeine for 24 hours or staurosporine (positive control) for 3 hours and analyzed with immunoblotting for levels of caspase-3 and cleaved caspase-3. (E) After PC12D cells were treated with 0, 1, 2.5, 5 or 10 mM caffeine with or without 1, 3 or 5 mM 3MA for 24 hours, cell viability was measured by trypan blue dye exclusion assay. (F) PC12D cells were transfected with control siRNA or siRNAs targeting Atg7. Forty eight hours later, they were treated with 0, 1, 2.5 or 10 mM caffeine for 24 hours and mitochondrial membrane potential was analyzed using JC-1. The knockdown effects on *Atg7* were confirmed by immunoblotting using antibodies against *Atg7* and actin. Data are the means of triplicate experiments. Error bars, S.D. NS, not significant; *p < 0.05; **p < 0.01; ***p < 0.001.

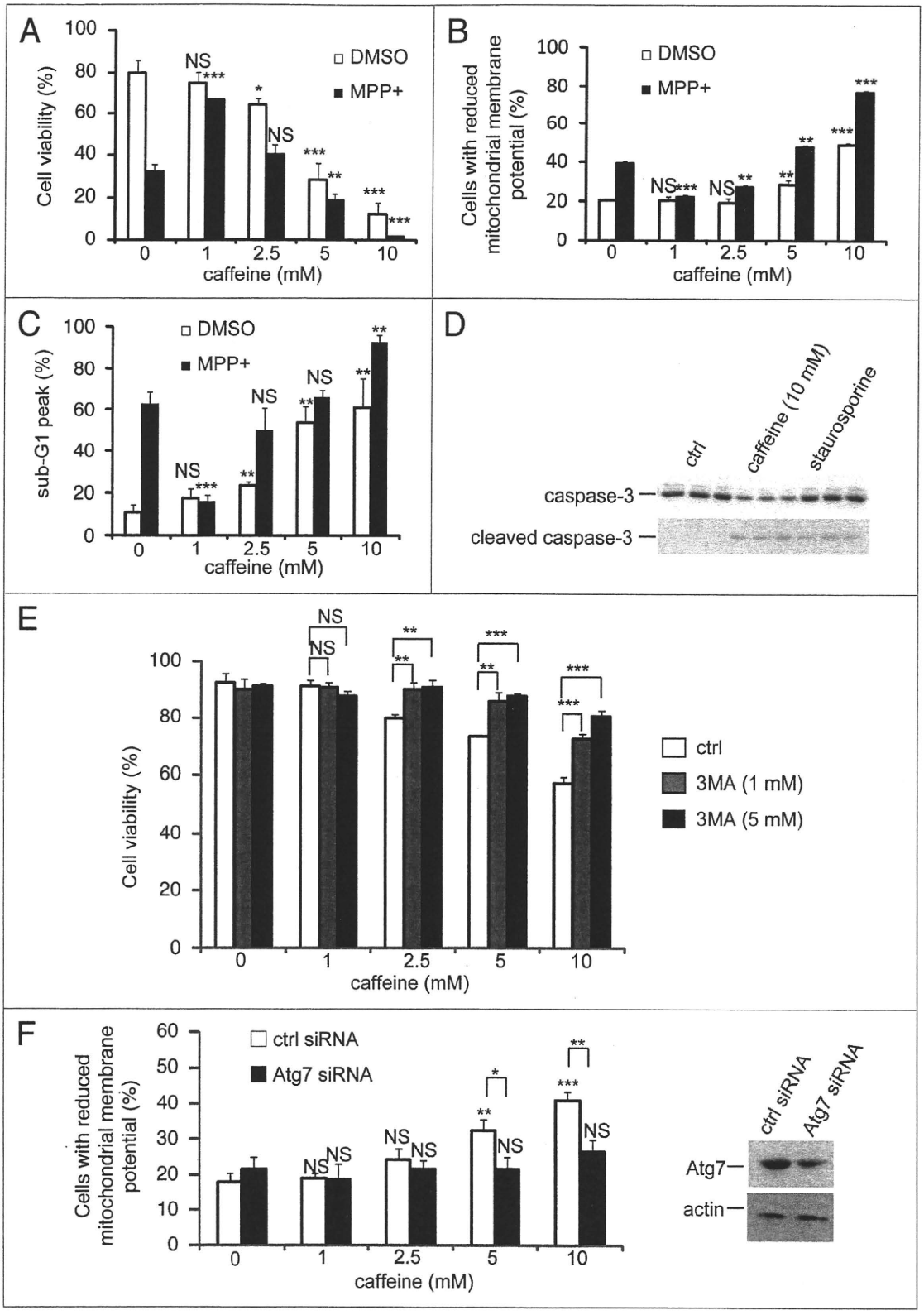

Figure 6. For figure legend, see page 183.

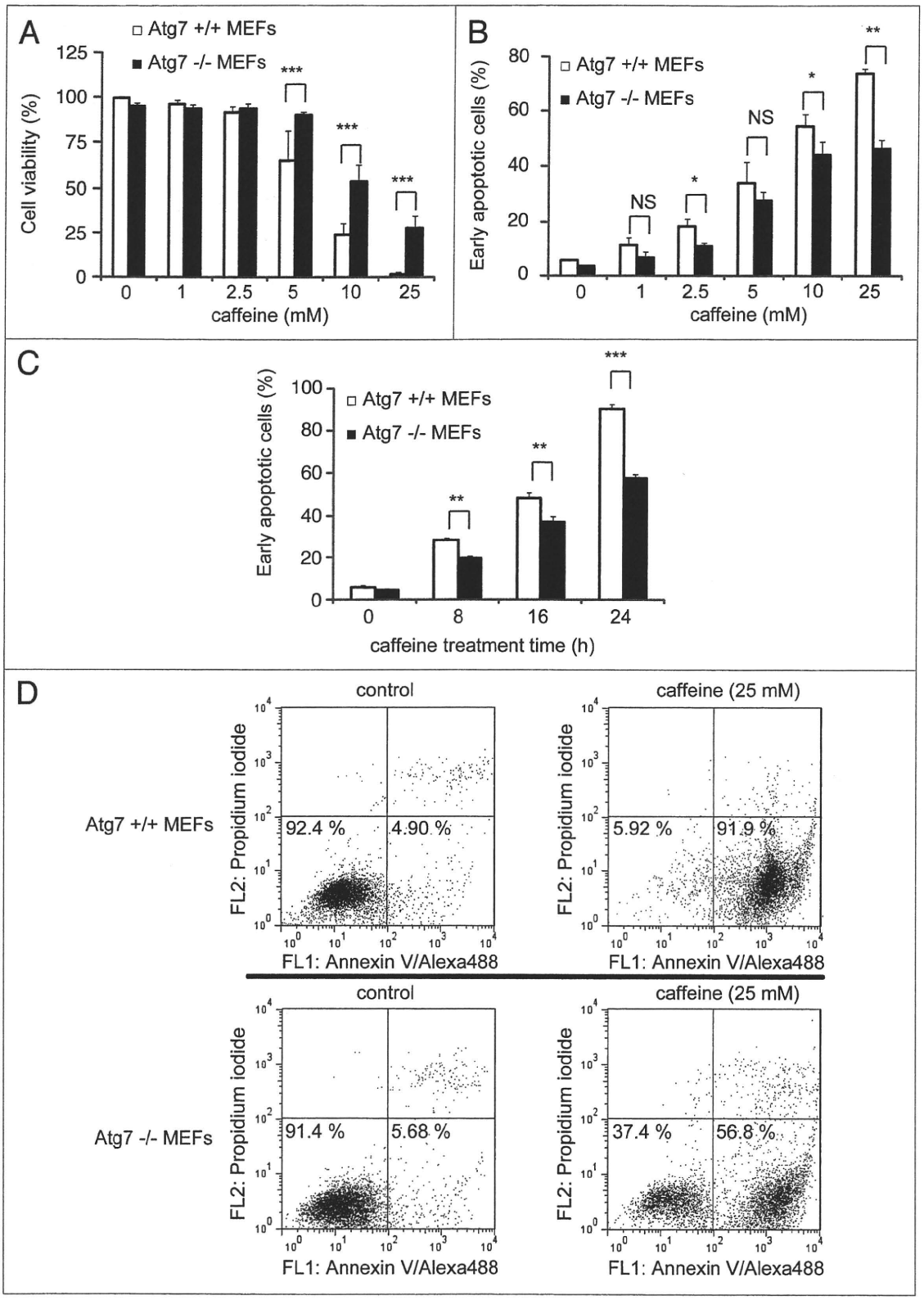

Figure 7. Cells without *Atg7* expression are more resistant to caffeine-induced apoptosis. (A) After *Atg7*$^{+/+}$ or $^{-/-}$ mouse embryonic fibroblasts (MEFs) were treated with 0, 1, 2.5, 5, 10, 25 mM caffeine for 24 hours, the cell viability was measured by trypan blue dye exclusion assay. Data are the means of triplicate experiments. (B–D) Fluorescence-activated cell-sorting analysis for annexin V/propidium iodide (PI). *Atg7*$^{+/+}$ or $^{-/-}$ MEFs were cultured with various concentrations of caffeine for 24 hours (B) or with 25 mM caffeine for various times (0, 8, 16 or 24 hours) (C and D). Annexin V/PI staining was subsequently performed to assess early or late apoptosis and necrosis. 5 x 10^3 cells were analyzed by flow cytometry and the percentage of early apoptotic cells (annexin V-positive and PI-negative cells, the lower right region in (D) was determined). Data are the means of triplicate experiments. Error bars, SD. NS, not significant; *$p < 0.05$; **$p < 0.01$; ***$p < 0.001$.

flow cytometry using FACScan and CellQuest software (BD Biosciences).

Compounds. Compounds used included caffeine (Wako, 031-06792), E64d (Sigma, E8640), pepstatin A (Sigma, P5318), rapamycin (LC Laboratories, R5000), CCI-779 (Selleck Chemicals, S1044), MPP^+ (Sigma, M0896), bafilomycin A1 (Sigma, B1793), 3-methyladenine (Sigma, M9281), insulin (Sigma, I0516), U0126 (Sigma, U120), Akt1/2 inhibitors (Sigma, A6730), staurosporine (Cell Signaling Technology, 9953) and DMSO (Sigma, D2650).

Plasmid DNAs. Myrystoylated Akt (21–151), a constitutively active form of Akt, was purchased from Millipore.

siRNA knockdown experiments. PC12D cells were transfected with rat Atg7 siRNAs (Invitrogen, 10620318-9) using Lipofectamine RNAiMAX (Invitrogen, 13778-075) according to the manufacturer's protocol.

Western blotting. Cell pellets were lysed on ice in RIPA buffer for 20 minutes in the presence of protease inhibitor (Roche). Western blotting was performed according to a previously published report.[42] The antibodies used were as follows: anti-p70 ribosomal protein (Cell Signaling Technology, 2708), anti-ribosomal protein (Cell Signaling Technology, 2217), anti-4E-BP1 (Cell Signaling Technology, 9452), anti-Akt (Cell Signaling Technology, 9272), anti-p44/42 MAP kinase (Cell Signaling Technology, 9102), anti-phospho-p70 ribosomal protein (Thr389) (Cell Signaling Technology, 9205), anti-phospho-S6 ribosomal protein (Ser235/236) (Cell Signaling Technology, 2211), anti-phospho-4E-BP1 (Thr37/46) (Cell Signaling Technology, 9459), anti-phospho-p44/p42 MAPK (Thy202/Tyr204) (Cell Signaling Technology, 9101), anti-Atg7 (Cell Signaling Technology, 2631), anti-phospho-Akt (Cell Signaling Technology, 4060), anti-actin (Millipore, clone C4), anti-LC3 (MBL, clone 4E12), anti-p62 (Progen Biotechnik, GP62-C) antibodies. Antibody signals were enhanced with chemifluorescent methods from GE HealthCare.

Immunofluorescent microscopy. Cells were embedded with 4% paraformaldehyde for 20 minutes. Following this, they were permeabilized with 0.1% Triton-X in 1x PBS. After incubation with 10% FBS and 1% bovine serum albumin in 1x PBS for 30 minutes, cells were immunostained with anti-LC3B (x500) (Sigma, L7543), anti-LAMP2 (x50) (Development Studies Hybridoma Bank, clone H4B4) overnight and incubated with anti-rabbit IgG tagged with AlexaFluor 488 or anti-mouse IgG tagged with AlexaFluor 546 for 1 hour. The cover slips were embedded with VectaShield, stained with DAPI and images were acquired on a Zeiss LSM510 META confocal microscope (63 x 1.4 NA) or a Leica TCS SP5 confocal microscope at room temperature using Zeiss LSM510 v.3.2 software or Leica LAS AF software. Adobe Photoshop 7.0 (Adobe Systems Inc.) was used for subsequent image processing. For colocalization assay in HeLa cells, an appropriate confocal image was taken with Leica LAS AF software. Then, these images were analyzed automatically with the ImageJ "Colocalization" Plugin (Settings: Each threshold: 25, Ratio: 75%) followed by "Analyze particles" (Settings: threshold 25; Pixel: 1) between endogenous LC3 positive and LAMP2 vesicles. Experiments were done in triplicate at least twice.

Quantification of cells with GFP-LC3 vesicles. HeLa cells stable expressing GFP-LC3 were treated with various concentrations of caffeine for 24 or 48 hours and then fixed as described above. Analyses in triplicate were done for counting the proportion of GFP-positive cells with GFP-LC3 vesicles as previously described in reference 43.

Electron microscopy. SH-SY5Y cells treated with various concentrations of caffeine were prefixed in 2% glutaraldehyde in PBS at 4°C, treated with 1% OsO_4 for 3 hours at 4°C, dehydrated in a graded series of ethanol and flat embedded in epon. Ultra-thin sections were doubly stained with uranyl acetate and observed using a JEOL JEM-2000EX electron microscopy at 80 kV.

Statistical analysis. Densitometry analysis was performed using ImageJ 1.43 on immunoblots from three independent experiments. A t-test was performed with SYSTAT software (Hulinks).

Acknowledgements

We thank Dr. Takashi Ueno (Department of Biochemistry, Juntendo University) for critical comments and Drs. Masaaki Komatsu and Yu-Shin Sou for providing *Atg7*$^{+/+}$ and $^{-/-}$ MEFs. We are very grateful for a grant from Hayashi Memorial Foundation for Female Natural Scientists (Y.S.), the Grant-in-Aid for Young Scientists (B) (S. Saiki and F. Sato), grants from the All Japan Coffee Association (S. Saiki), the Takeda Scientific Foundation (S. Saiki) and the Nagao Memorial Fund (S. Saiki).

Note

Supplementary materials can be found at:
www.landesbioscience.com/journals/autophagy/article/14074

References

1. Bode AM, Dong Z. The enigmatic effects of caffeine in cell cycle and cancer. Cancer Lett 2007; 247:26-39.
2. Jang MH, Shin MC, Kang IS, Baik HH, Cho YH, Chu JP, et al. Caffeine induces apoptosis in human neuroblastoma cell line SK-N-MC. J Korean Med Sci 2002; 17:674-8.
3. Gururajanna B, Al-Katib AA, Li YW, Aranha O, Vaitkevicius VK, Sarkar FH. Molecular effects of taxol and caffeine on pancreatic cancer cells. Int J Mol Med 1999; 4:501-7.
4. Qi W, Qiao D, Martinez JD. Caffeine induces TP53-independent G(1)-phase arrest and apoptosis in human lung tumor cells in a dose-dependent manner. Radiat Res 2002; 157:166-74.
5. Mizushima N, Levine B, Cuervo AM, Klionsky DJ. Autophagy fights disease through cellular self-digestion. Nature 2008; 451:1069-75.
6. Rubinsztein DC. The roles of intracellular protein-degradation pathways in neurodegeneration. Nature 2006; 443:780-6.
7. Eisenberg-Lerner A, Bialik S, Simon HU, Kimchi A. Life and death partners: apoptosis, autophagy and the cross-talk between them. Cell Death Differ 2009; 16:966-75.
8. Espert L, Denizot M, Grimaldi M, Robert-Hebmann V, Gay B, Varbanov M, et al. Autophagy is involved in T cell death after binding of HIV-1 envelope proteins to CXCR4. J Clin Invest 2006; 116:2161-72.
9. Foukas LC, Daniele N, Ktori C, Anderson KE, Jensen J, Shepherd PR. Direct effects of caffeine and theophylline on p110delta and other phosphoinositide 3-kinases. Differential effects on lipid kinase and protein kinase activities. J Biol Chem 2002; 277:37124-30.
10. Kudchodkar SB, Yu Y, Maguire TG, Alwine JC. Human cytomegalovirus infection alters the substrate specificities and rapamycin sensitivities of raptor- and rictor-containing complexes. Proc Natl Acad Sci USA 2006; 103:14182-7.
11. Winter G, Hazan R, Bakalinsky AT, Abeliovich H. Caffeine induces macroautophagy and confers a cytocidal effect on food spoilage yeast in combination with benzoic acid. Autophagy 2008; 4:28-36.

12. Rubinsztein DC, Cuervo AM, Ravikumar B, Sarkar S, Korolchuk V, Kaushik S, Klionsky DJ. In search of an "autophagomometer". Autophagy 2009; 5:585-9.
13. Tanida I, Ueno T, Kominami E. LC3 and Autophagy. Methods Mol Biol 2008; 445:77-88.
14. Kabeya Y, Mizushima N, Ueno T, Yamamoto A, Kirisako T, Noda T, et al. LC3, a mammalian homologue of yeast Apg8p, is localized in autophagosome membranes after processing. EMBO J 2000; 19:5720-8.
15. Yamamoto A, Tagawa Y, Yoshimori T, Moriyama Y, Masaki R, Tashiro Y. Bafilomycin A1 prevents maturation of autophagic vacuoles by inhibiting fusion between autophagosomes and lysosomes in rat hepatoma cell line, H-4-II-E cells. Cell Struct Funct 1998; 23:33-42.
16. Mizushima N, Yoshimori T, Levine B. Methods in mammalian autophagy research. Cell 140:313-26.
17. Hanahan D, Weinberg RA. The hallmarks of cancer. Cell 2000; 100:57-70.
18. Ikenoue T, Hong S, Inoki K. Monitoring mammalian target of rapamycin (mTOR) activity. Methods Enzymol 2009; 452:165-80.
19. Sinn B, Tallen G, Schroeder G, Grassl B, Schulze J, Budach V, Tinhofer I. Caffeine confers radiosensitization of PTEN-deficient malignant glioma cells by enhancing ionizing radiation-induced G_1 arrest and negatively regulating Akt phosphorylation. Mol Cancer Ther 9:480-8.
20. Sarkaria JN, Busby EC, Tibbetts RS, Roos P, Taya Y, Karnitz LM, Abraham RT. Inhibition of ATM and ATR kinase activities by the radiosensitizing agent, caffeine. Cancer Res 1999; 59:4375-82.
21. Inoki K, Li Y, Xu T, Guan KL. Rheb GTPase is a direct target of TSC2 GAP activity and regulates mTOR signaling. Genes Dev 2003; 17:1829-34.
22. Inoki K, Li Y, Zhu T, Wu J, Guan KL. TSC2 is phosphorylated and inhibited by Akt and suppresses mTOR signalling. Nat Cell Biol 2002; 4:648-57.
23. Garami A, Zwartkruis FJ, Nobukuni T, Joaquin M, Roccio M, Stocker H, et al. Insulin activation of Rheb, a mediator of mTOR/S6K/4E-BP signaling, is inhibited by TSC1 and 2. Mol Cell 2003; 11:1457-66.
24. Muise-Helmericks RC, Grimes HL, Bellacosa A, Malstrom SE, Tsichlis PN, Rosen N. Cyclin D expression is controlled post-transcriptionally via a phosphatidylinositol-3-kinase/Akt-dependent pathway. J Biol Chem 1998; 273:29864-72.
25. Degtyarev M, De Maziere A, Orr C, Lin J, Lee BB, Tien JY, et al. Akt inhibition promotes autophagy and sensitizes PTEN-null tumors to lysosomotropic agents. J Cell Biol 2008; 183:101-16.
26. Wan X, Harkavy B, Shen N, Grohar P, Helman LJ. Rapamycin induces feedback activation of Akt signaling through an IGF-1R-dependent mechanism. Oncogene 2007; 26:1932-40.
27. Sun SY, Rosenberg LM, Wang X, Zhou Z, Yue P, Fu H, Khuri FR. Activation of Akt and eIF4E survival pathways by rapamycin-mediated mammalian target of rapamycin inhibition. Cancer Res 2005; 65:7052-8.
28. O'Reilly KE, Rojo F, She QB, Solit D, Mills GB, Smith D, et al. mTOR inhibition induces upstream receptor tyrosine kinase signaling and activates Akt. Cancer Res 2006; 66:1500-8.
29. Cirstea D, Hideshima T, Rodig S, Santo L, Pozzi S, Vallet S, et al. Dual inhibition of akt/mammalian target of rapamycin pathway by nanoparticle albumin-bound-rapamycin and perifosine induces antitumor activity in multiple myeloma. Mol Cancer Ther 2010; 9:963-75.
30. Aoki H, Takada Y, Kondo S, Sawaya R, Aggarwal BB, Kondo Y. Evidence that curcumin suppresses the growth of malignant gliomas in vitro and in vivo through induction of autophagy: role of Akt and extracellular signal-regulated kinase signaling pathways. Mol Pharmacol 2007; 72:29-39.
31. Ellington AA, Berhow MA, Singletary KW. Inhibition of Akt signaling and enhanced ERK1/2 activity are involved in induction of macroautophagy by triterpenoid B-group soyasaponins in colon cancer cells. Carcinogenesis 2006; 27:298-306.
32. Rubinsztein DC, Gestwicki JE, Murphy LO, Klionsky DJ. Potential therapeutic applications of autophagy. Nat Rev Drug Discov 2007; 6:304-12.
33. Ravikumar B, Vacher C, Berger Z, Davies JE, Luo S, Oroz LG, et al. Inhibition of mTOR induces autophagy and reduces toxicity of polyglutamine expansions in fly and mouse models of Huntington disease. Nat Genet 2004; 36:585-95.
34. Kotake Y, Ohta S. MPP^+ analogs acting on mitochondria and inducing neuro-degeneration. Curr Med Chem 2003; 10:2507-16.
35. Hagan MP, Hopcia KL, Sylvester FC, Held KD. Caffeine-induced apoptosis reveals a persistent lesion after treatment with bromodeoxyuridine and ultraviolet-B light. Radiat Res 1997; 147:674-9.
36. Efferth T, Fabry U, Glatte P, Osieka R. Expression of apoptosis-related oncoproteins and modulation of apoptosis by caffeine in human leukemic cells. J Cancer Res Clin Oncol 1995; 121:648-56.
37. Shinomiya N, Takemura T, Iwamoto K, Rokutanda M. Caffeine induces S-phase apoptosis in cis-diamminedichloroplatinum-treated cells, whereas cis-diamminedichloroplatinum induces a block in G_2/M. Cytometry 1997; 27:365-73.
38. Lau CC, Pardee AB. Mechanism by which caffeine potentiates lethality of nitrogen mustard. Proc Natl Acad Sci USA 1982; 79:2942-6.
39. Takagi M, Shigeta T, Asada M, Iwata S, Nakazawa S, Kanke Y, et al. DNA damage-associated cell cycle and cell death control is differentially modulated by caffeine in clones with p53 mutations. Leukemia 1999; 13:70-7.
40. Ormerod MG, Collins MK, Rodriguez-Tarduchy G, Robertson D. Apoptosis in interleukin-3-dependent haemopoietic cells. Quantification by two flow cytometric methods. J Immunol Methods 1992; 153:57-65.
41. Kawatani M, Uchi M, Simizu S, Osada H, Imoto M. Transmembrane domain of Bcl-2 is required for inhibition of ceramide synthesis, but not cytochrome *c* release in the pathway of inostamycin-induced apoptosis. Exp Cell Res 2003; 286:57-66.
42. Kawajiri S, Saiki S, Sato S, Sato F, Hatano T, Eguchi H, Hattori N. PINK1 is recruited to mitochondria with parkin and associates with LC3 in mitophagy. FEBS Lett 2010; 584:1073-9.
43. Sarkar S, Davies JE, Huang Z, Tunnacliffe A, Rubinsztein DC. Trehalose, a novel mTOR-independent autophagy enhancer, accelerates the clearance of mutant huntingtin and alpha-synuclein. J Biol Chem 2007; 282:5641-52.

Neuroscience Letters 481 (2010) 88–91

Contents lists available at ScienceDirect

Neuroscience Letters

journal homepage: www.elsevier.com/locate/neulet

Zonisamide reduces cell death in SH-SY5Y cells via an anti-apoptotic effect and by upregulating MnSOD

Sumihiro Kawajiri[a,1], Yutaka Machida[b,1], Shinji Saiki[a], Shigeto Sato[a], Nobutaka Hattori[a,*]

[a] Department of Neurology, Juntendo University School of Medicine, 2-1-1 Hongo, Bunkyo-ku, Tokyo, 113-8421, Japan
[b] Department of Neurology, Juntendo University Nerima Hospital, 3-1-10 Takanodai, Nerima-ku, Tokyo, 177-0033, Japan

ARTICLE INFO

Article history:
Received 15 April 2010
Received in revised form 8 June 2010
Accepted 21 June 2010

Keywords:
Zonisamide
Apoptosis
Manganese superoxide dismutase
Parkinson's disease

ABSTRACT

Zonisamide, originally known as an antiepileptic drug, has been approved in Japan as adjunctive therapy with levodopa for the treatment of Parkinson's disease (PD). Although zonisamide reduces neurotoxicity, the precise mechanism of this action is not known. Here, we show that zonisamide increases cell viability in SH-SY5Y cells via an anti-apoptotic effect and by upregulating levels of manganese superoxide dismutase (MnSOD). These results would give us novel evidences of PD treatment.

Parkinson's disease (PD) is the second most common neurodegenerative disease characterized by pronounced loss of dopaminergic neurons in the substantia nigra pars compacta. At present, there is no known treatment to suppress the progression of this cell death and the goal of current therapies is only to alleviate symptoms. New therapies are, therefore, required to delay disease progression and to improve the long-term prognosis of PD. Mitochondrial dysfunction due to oxidative stress has been proposed as a major factor in the pathogenesis of PD [3,22] and reduced activity in mitochondrial complex I is associated with PD [13,22]. After complex I blockade with 1-methyl-4-phenyl-1,2,3,6-tetrahydropyridine (MPTP) in mice, there is a time-dependent and region-specific activation of mitochondrial cytochrome c, which activates caspase-9 and -3, resulting in apoptosis [20].

Zonisamide, originally known as an anticonvulsant agent, has been approved in Japan as adjunctive therapy with levodopa for patients with PD [15,16]. The mechanism of zonisamide to improve Parkinsonism has been reported to modify the turnover and synthesis of dopamine (DA) [18,28]. Moreover, it has been recently reported that zonisamide attenuates MPTP-induced and 6-hydroxydopamine (6-OHDA)-induced neurotoxicity and dopaminergic neuron-specific oxidative stress in mice [1,2,29,30]. Although zonisamide is likely to delay the progress of PD, the exact mechanism of its action remains unclear.

In this study, we show that zonisamide increases the viability of differentiated SH-SY5Y cells by inhibiting activation of proapoptotic molecules and upregulating levels of manganese superoxide dismutase (MnSOD), also known as superoxide dismutase-2 (SOD2).

The following antibodies were used in this study: anti-caspase-3 antibody (rabbit), anti-caspase-9 antibody (rabbit), and anti-phospho-SAPK/JNK (Thr183/Tyr185) antibody (rabbit) were obtained from Cell Signaling Technology. Anti-actin antibody (mouse) was from Millipore. Anti-MnSOD antibody (rabbit) was from Upstate.

SH-SY5Y cells were grown in Dulbecco's modified Eagle's medium (DMEM) (Sigma) supplemented with 10% fetal bovine serum (FBS) (Sigma) and 1% penicillin–streptomycin (Invitrogen-GIBCO) at 37 °C and 5% CO_2. To induce cell differentiation, SH-SY5Y cells were incubated in complete medium plus 10 μM *all-trans* retinoic acid (Sigma) for 72 h. For pharmacological studies, zonisamide (Dainippon Sumitomo Pharma Co.), staurosporine (Cell Signaling Technology), 1-methyl-4-phenyl-pyridium ion (MPP^+) (Sigma), and dopamine hydrochloride (Sigma) were added at indicated times and concentrations.

Cell viability was assessed by the WST assay; the ability of mitochondrial activity to reduce 2-(2-methoxy-4-nitrophenyl)-3-(4-nitrophenyl)-5-(2,4-disulfophenyl)-2H-tetrazolium monosodium salt (WST-8) to formazan using the Cell Counting Kit-8 (Dojindo, Kumamoto, Japan), according to the manufacturer's instructions.

TdT-mediated dUTP-biotin nick-end labeling (TUNEL) staining was performed using the *In situ* Cell Death Detection Kit, Fluorescein (Roche) according to the manufacturer's instructions. Cells were then mounted with Vectashield containing DAPI (Vector Lab-

* Corresponding author. Tel.: +81 3 3813 3111; fax: +81 3 5800 0547.
E-mail address: nhattori@juntendo.ac.jp (N. Hattori).
[1] Joint first authors.

0304-3940/$ – see front matter © 2010 Elsevier Ireland Ltd. All rights reserved.
doi:10.1016/j.neulet.2010.06.058

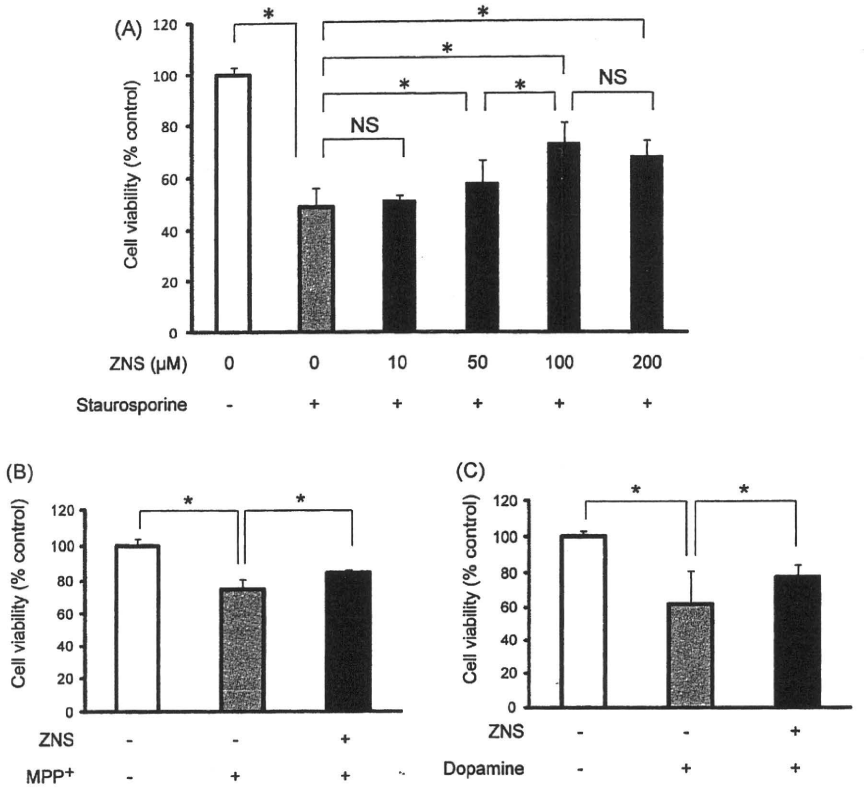

Fig. 1. Zonisamide increases cell viability. (A) Differentiated SH-SY5Y cells were treated with staurosporine (0.2 μM) for 5 h before the WST assay was performed, with or without 24 h treatment with various concentrations of zonisamide. Absorbance at 450 nm was measured. (B) and (C) MPP^+ (500 μM) treatment for 24 h (B), or dopamine (50 μM) treatment for 24 h (C). WST assay was performed with or without 24 h treatment with zonisamide (100 μM). ZNS, zonisamide. $^*p < 0.05$. NS, non-significant. Error bars indicate standard deviation of at least five experiments.

oratories, Burlingame, CA, USA) and examined using a fluorescence microscope (BZ-9000; KEYENCE, Japan). Image processing was performed using Adobe Photoshop CS3.

For immunoblot analysis, cells were lysed on ice in lysis buffer [10 mM Tris–HCl (pH 7.5), 150 mM NaCl, 1 mM EDTA, 1% NP-40, and protease inhibitors (complete, Mini, EDTA-free, Roche Applied Science)]. Cell lysates were mixed with NuPAGE 4× LDS sample buffer (Invitrogen). The samples were separated by SDS-PAGE, and proteins were transferred to polyvinylidene fluoride (PVDF) membranes (Millipore). The membranes were blocked with 5% non-fat milk (BD Difco) in Tris-buffered saline containing 0.05% Tween20 (TBS-T) and then incubated overnight at 4 °C with the primary antibody. The membranes were incubated for 1 hour at room temperature with the secondary antibody and visualized using ECL plus reagent (GE Health Care Bio-Sciences) or with Western Lightning (Perkin Elmer-Cetus). After scanning the images, the intensity of each immunoreactive band was estimated by densitometric quantification using ImageJ 1.42 software.

We first examined the effects of zonisamide on the viability of differentiated human neuroblastoma cells (SH-SY5Y cells), which are dopaminergic and can differentiate into neuronal-like phenotypes when treated for 3–5 days with retinoic acid (10 μM). Differentiation is accompanied by the arrest of cell proliferation and increased dopamine metabolism [17,24]. We assessed cell viability using the WST-8 assay [11,25]. In this assay, the tetrazolium salt, WST-8, is cleaved to formazan by a complex cellular mechanism that occurs primarily at the cell surface. This bioreduction is mostly dependent on the production of glycolytic NAD(P)H in viable cells. Therefore, the amount of formazan dye formed directly correlates to the number of metabolically active cells. For staurosporine-treated cells, treatment with zonisamide at 50 μM or over induced an increase of cell viability, with the greatest effect being at 100 μM (Fig. 1A). Subsequent experiments were, therefore, performed using 100 μM zonisamide. Various PD-cellular models have been established using neurotoxins that cause neurotoxicity towards dopaminergic neurons, such as MPTP, DA, rotenone and paraquat [4,5,7,10,23]. Therefore, we next performed similar experiments in the presence of MPP^+ and DA. Zonisamide treatment also prevented subsequence of cell death following MPP^+-treatment (Fig. 1B) and DA-treatment (Fig. 1C). These results indicate that zonisamide has neuroprotective effects in PD-cellular models.

Apoptosis is a major cell death pathway in PD and other neurodegenerative diseases [19]. To investigate the mechanisms by which zonisamide exerts its cytoprotective effects, we examined whether the zonisamide-induced increase of cell viability occurs via an anti-apoptotic effect. We assessed apoptosis in differentiated, staurosporine-treated SH-SY5Y cells using TUNEL staining. As expected, the proportion of TUNEL-positive cells was reduced by zonisamide treatment compared with untreated cells (Fig. 2A and B). To confirm the anti-apoptotic effect of zonisamide, we also examined proapoptotic molecules [caspase-9, -3, and phospho-c-Jun N-terminal kinase (p-JNK)] in differentiated SH-SY5Y cells. Zonisamide treatment reduced the levels of cleaved caspase-9, -3, and p-JNK (Fig. 2C and D). Cleaved caspase-9 is produced in response to mitochondrial damage and the production of cleaved caspase-3 is downstream of cleaved caspase-9. Activation of JNK by reactive oxygen species (ROS) is critical for the induction of apoptosis in neuronal cells [21,27]. Our results suggest that zonisamide blocks the activation of proapoptotic molecules in differentiated SH-SY5Y cells. Also, although PD pathogenesis has been associated with both an excess and a deficiency of autophagic activity [9,26], zonisamide had no effect on autophagic activity because no alteration in the LC3-II/actin ratio, an indicator of autophagic activity, was observed (data not shown).

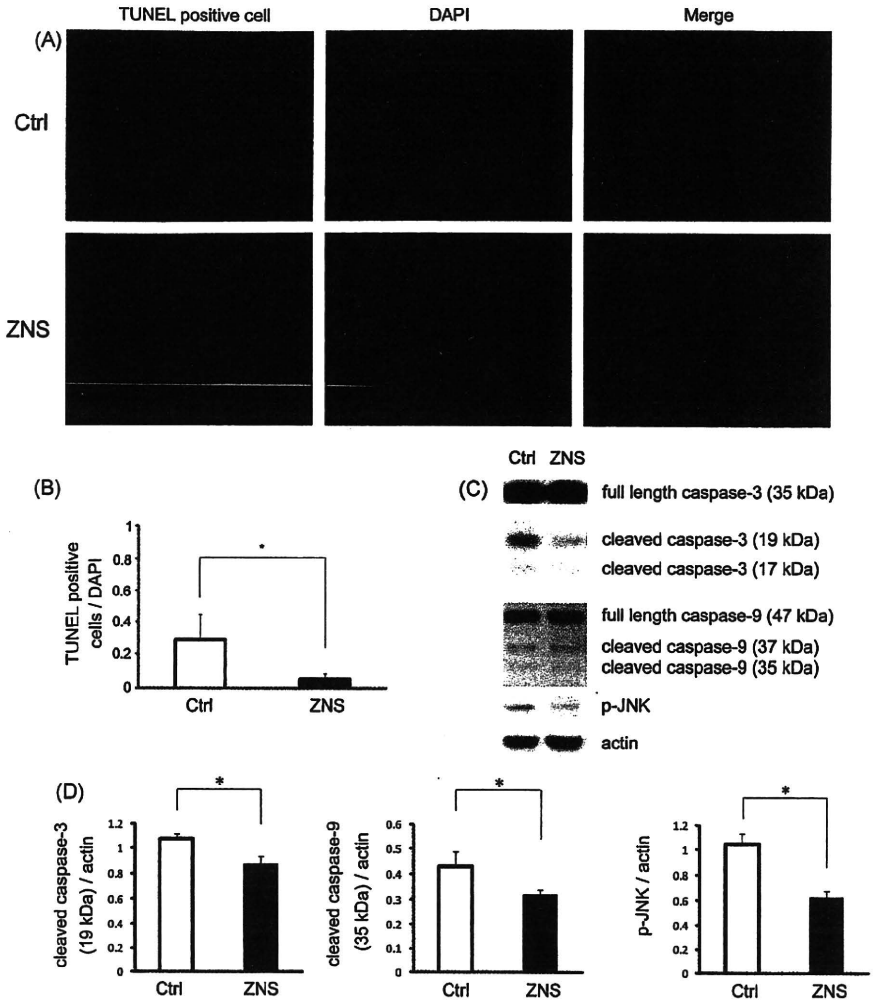

Fig. 2. Zonisamide has anti-apoptotic effects. Differentiated SH-SY5Y cells were treated with staurosporine (0.2 μM) for 3 h, with or without of 24 h treatment with zonisamide (100 μM). (A) TUNEL staining. TUNEL-positive cells are in red. DAPI stained nuclei are in blue. (B) Quantification of TUNEL staining: ratio of TUNEL-positive cells to DAPI stained nuclei is shown. (C) Full length caspase-3, -9, Cleaved caspase-3, -9, and p-JNK levels were analyzed by western blotting. The bottom panel shows actin as a loading control. (D) Quantification of (C): ratios of cleaved caspase-3, -9, and p-JNK to actin are shown. $^*p < 0.05$. Error bars indicate standard deviation of at least three independent experiments. Ctrl, control. ZNS, zonisamide.

MnSOD over-expression attenuates MPTP toxicity and protects cells from apoptosis [12,31], while transgenic mice over-expressing MnSOD are more resistant to MPTP toxicity [8]. Based on the results presented in Figs. 1 and 2, we examined whether zonisamide treatment regulates MnSOD activity. We assayed the effects of zonisamide treatment on MnSOD levels in differentiated, staurosporine-treated SH-SY5Y cells. Zonisamide treatment induced an increase in MnSOD levels (Fig. 3A and B). MnSOD is an antioxidant localized in mitochondria and represents a major defense against superoxide free radicals produced in mitochondria. Zonisamide is also known to scavenge hydroxyl radicals and nitric oxide radicals in cell-free systems, which is consistent with our data [2,14]. Although NF-κB is known to be upstream of MnSOD [6], zonisamide treatment did not affect NF-κB levels (data not shown). We did not investigate the zonisamide-induced mechanism of MnSOD upregulation.

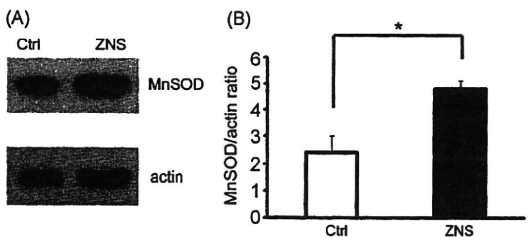

Fig. 3. Zonisamide upregulates levels of MnSOD. (A) Manganese superoxidase dismutase (MnSOD) levels in differentiated SH-SY5Y cells treated with staurosporine (0.2 μM) for 3 h with or without 24 h treatment with zonisamide (100 μM) were analyzed by western blotting. The bottom panel shows actin as a loading control. (B) Quantification of MnSOD western blot: ratio of MnSOD to actin is shown; $^*p < 0.05$. Error bars indicate standard deviation of at least three independent experiments. Ctrl, control. ZNS, zonisamide.

In the present study, we provide several lines of evidence showing that zonisamide increased neuronal cell viability via effects on apoptosis and oxidative stress. This interpretation is based on: (1) zonisamide increased cell viability of cells treated with staurosporine and of cells in PD-cellular models. (2) Zonisamide reduced the number of TUNEL-positive cells and the levels of proapoptotic molecules. (3) Zonisamide upregulated levels of MnSOD.

Previous studies have shown that zonisamide significantly attenuates MPTP-induced neurotoxicity by inhibiting microglial activation or 6-OHDA-induced neurotoxicity by increasing glutathione (GSH) via enhancing astroglial cysteine transport system and astroglial proliferation [1,29,30]. However, the direct pharmacological effects on neurons has not been fully investigated. Consistent with previous reports that have investigated cytoprotective effects in PD-cellular models, we demonstrated that